Dynamics of early stages of nose morphogenesis

Vincent Fleury

Dynamics of early stages of nose morphogenesis

Vincent Fleury[1]

Laboratoire Matière et Systèmes Complexes, Université de Paris Cité/CNRS UMR 7057

10 rue Alice Domont et Léonie Duquet, Paris 75013, France.

Corresponding author e-mail : vincent.fleury@u-paris.fr

[1]Orcid : **0000-0002-4716-0517**

Abstract

The formation of sensory organs is an important developmental and evolutionary question. In the context of regenerative medicine also, it is important to know as accurately as possible how sensory organs form. The formation of ears, eyes or nose, stem presumably from tissue thickenings called *placodes* [1,2] which become these organs after processes termed *inductions*. However, the origin of the placodes, the mechanism of induction, and the overall face organization are not understood. Recently, it has been suggested that there is a physical principle to face organization. Indeed, it has been shown that there exists a pattern of rings and rays in the early blastula which defines the position of face landmarks, especially the ears and eyes [3,4]. Tensions in the sectors defined by the intersections of the said rings and rays create the actual face features. I report here that a similar situation exists for the nose. This explains the robustness of face formation in the chordates phylum. By studying nasal pit formation in the chicken embryo by Time-Lapse (T-L) video microscopy, I show that the nasal placode originates in a narrow sector deformed by tension forces following the biaxial pattern of rings and rays mentioned above. Cells align in the pattern and exert organized forces. Further contractions of the pattern contribute to inducing the nasal pit. The observation of the early pre-pattern of lines which locks the facial features explains readily a number of facts regarding sensory organs. Especially the existence of a lacrimal canal between the eye and the nose [5], or of a slit connecting the nose to the mouth, the correlation between nose, mouth and eye morphogenesis [6], the presence of shallow valleys on the nasal and optic vesicles, the medio-lateral asymmetry of nostrils with often a bent slit [7], the uneven number of nostrils in many fish [8] and possibly the transition between agnatha and gnathostomes [9] : all appear under this light, geometrically straightforward.

Main

Understanding the formation of organs is an important scientific endeavor. There exist several types of organs. Sensory organs of the head are particular in that they play a crucial role in

our humanity : they are partly external, we sense the world with them, and they define our identity (an identity photography is a portrait). The biology of the face and of the sensory organs is therefore of great importance at symbolic, psychological and medical levels. In the contexts of pediatric surgery or of regenerative medicine, it is important to understand the formation of these organs with precision. The eye is certainly the organ which has attracted the highest interest, being an endless source of debate about biological complexity [10,11]. We likely find next the ears [12,13], and finally, the *parent pauvre* of sensory organ studies is the nose [14,15].

However, it is well known classically that embryos form in two steps [16] : first, immediately after fertilization, a phase of *segmentation*, during which the zygote is regularly cleaved and called a *morula*. When the number of cells reaches a few thousands, the chicken embryo, although stratified, is flat, and it is called a *blastodisc*. Then this bastodisc rolls-up, and the embryo body acquires a 3D form as we know it, made of folded tissue. It is generally considered that sensory organs form from "placodes" [1,2], which are paired ectodermal thickenings located around the presumptive neural territory. One finds descriptions of placodes in which such organ precursors are already positioned, at the earliest embryonic stages, in the form of round territories. However, during development, embryonic tissues undergo deformations of an extraordinary complexity [16-19] such that there is no reason *a priori* to expect round placodes, visible shortly before organ formation, to originate in anything like a round patch of tissue, already existing at the blastula stage. Moreover, nasal pits are rarely round, as for example in sharks (Fig. 1A Top left) or rays (Fig. 1A Top Right). In many animals such as dogs they exhibit a striking bent slit pattern [7] (Fig. 1A Bottom right), which can hardly be explained by a round placode. Moreover, not all animals have paired nasal pits. The agnatha, such as the lamprey (Fig. 1B Top) have a single nostril positionned on top of the head, along the median axis [20] ; conversely, many fish have paired incurrent and excurrent nostrils, which makes four nostrils [8] (Fig. 1B Bottom). A physicist naturally wonders whether there might be a mechanistic rationale, possibly some physical bifurcation, explaining trends in face organization, and in particular the presence of either a single nostril on top of the head, or two nostrils located on either side of the head, or four. All taxa which have bilateral nostrils present a high degree of homology, with most ancient taxa such as stingrays (Fig. 1A Top Right) or dogfish (Fig. 1A Middle Left) already having bilateral nostrils with a nasogenian groove[(1)] homologous to the one seen in humans (Fig. 1A Bottom Left). The robustness of facial organization, and the visible pattern of lines on the animal faces such as the nasogenian groove, suggests an underlying holistic physical principle to sensory organ formation, especially the nose. Such a general principle would generate a standard prepattern, with

[(1)] The main groove on the face on either side of the nose.

limited variability linked to tissue visco-elasticity in the spirit of D'Arcy Thompson's anamorphoses [21].

Alternatively, a sequence of chemical inductions in gradients, with whatever feedback loop, would be expected to generate a more arbitrary facial pattern. Stated otherwise : it seems from a physical point of view that the distribution of organs on the face is not at all arbitrary : something geometrical locks the nasal pits where they are, and nasal pits should not be expected anywhere else. It is indeed possible to position by art organs in aberrant positions ("ectopically"), by putting a bead soaked with some chemical under the ectoderm of an embryo; this assay has had a great success with limbs [22] and more recently with eyes [23]. However, this does not tell what is the "bead" in the physiological situation, and neither does it prove that nature would be able to position an organ anywhere arbitrarily by its own means. It has been shown recently that eye and ear placodes originate from bilateral trapezoidal sectors of tissue in the blastula which round off under the action of tension forces [3] to form the paired eyes and ears. I show hereafter that a similar phenomenon occurs for the nasal pits. Such a sector of tissue forming a hairpin is quite often directly visible on faces, under the nares, as for example on the seabream fish (*Pagrus pagrus* Fig. 1A, Middle Right) even in the absence of a nasogenian groove.

I use the chicken embryo as experimental model. The chicken head resembles fairly the mammalian head until formation of the beak begins (around day 10, HH stage 30; chicken embryo staging follows Hamilton and Hamburger stages [19]). Chicken embryology is made easier than mammal embryology by the fact that the embryos develop inside an egg. However, even in birds, observation of nasal development is difficult because the embryo develops inside a bag (the amnion, or bag of waters) with the ventral side down, and the head undergoes by the second day of development a pronounced forward flexure which contributes to hiding the presumptive nasal area and its surroundings (Supp. Fig. 1 Video 1, HH stages 15-17). This is why I have developed a sequence of dissection steps which allows one to observe the nasal area in detail, these steps are explained in the Supplementary Material (see Supp. Fig. 2). They end by a view of the embryo, from "profile" to "facial" depending on the chosen orientation. For early stages of development I use a more classical preparation, with embryos removed from the egg, rinsed and filmed *ex-ovo* on a flat Petri dish. All observations here after are in white light, with ordinary microscopes (no staining, no fluorescence, a double slit is used to enhance contrast see Supp. Material).

Results.

In vivo observations

During early stages of embryo morphogenesis (HH5), one classically observes a strong posterior pull of the median axis which forms the chord of the chordates, and triggers the roll up of

neural tissue to form a tube (see Video 2). During this event all anterior parts of the embryo are positioned [17,24]. If we look in detail the anterior area prior to neural roll-up, we observe the deformation by contraction of one anterior sector of tissue which defines the position of the mouth (Fig. 2A,B, Video 3). During chord extension, the contraction of the mouth sector continues, but other sectors become visible (Fig. 3A Video 4). One portion of sector is the presumptive eye territory, it has a horseshoe shape at this stage (Fig. 3B), bounded by the edge of the ventral ectoderm (see visible line boundary in Fig. 3B, arrow), which also constricts. During early neurulation, both the eye and the mouth sectors are stretched posteriorly by chord extension : they form visible elongated trapezoidal sector patterns (arrowheads in Fig. 3A, see also annotations in Video 4). At the beginning of neurulation (HH6-8), the eye territory rolls up, and it forms a bump locked by kinks or valleys in the neural tube, corresponding to the boundaries of the sector (Fig. 4, A, B, Videos 5, 6). The eye balloons out laterally from the neural tube in front of this sector (HH9-12, Fig. 4A, B Videos 7, 8, 9,10). The onset of lateral extension (HH9, Video 7) coincides with convergent-extension movements [25,26], which impart a dipolar rotatory movement (i.e. laterally, sideways and away from the body axis) to the eye territory [27] (Fig. 5A). Most importantly, the closure of the neural tube (HH10) coincides with a sudden dilation of the head features (Fig. 5B, see Video 9 and Video 11; in Video 11 the arrowhead points to the closing neural tube, the apex of the closure is called notopore). As the brain vesicles balloon out, the eye stalk extends (HH11-12, Videos 8, 10, 12 Fig. 5C, D Fig. 6). Flattened by brain dilation, the eye territory swerves its way towards the posterior direction where it forms an oblate capsule (the presumptive eye proper) (Fig. 6A,B Videos 12, 13), in Fig. 6A the arrows point to the posterior winding of the presumptive eye capsule. The buckling of the eye territory (HH15, Videos 1, 13) generates a propagating fold which is oriented towards the presumptive mouth corner. Stated otherwise, the eye invagination movement is biased and it has an almond shape oriented towards the mouth corner (this will be important later), corresponding in the initial situation to the kink pointed by the arrow in Fig. 2B.

The eye forms by contraction, delamination and a double invagination of the surface layer which gives the lens, and of the ectoderm of the eye capsule which forms the eye ball (see Video 8 in Ref. 3). These events have been documented before [3,4,28].

In the next 6 hours after eye formation, the nasal pit forms (Fig. 7A). Video 15 shows the formation of the nasal pit as seen under a binocular at Mag. 2X. We observe a non-linearity of nasal pit formation : a rapid snap contraction followed by a relaxation during nare invagination. Video 16 shows the moment of first appearance of a nare ridge at Mag. 3X, it shows a correlation between a contraction of the nasal territory, and onset of nare formation. Videos 17 shows the formation of the nasal pit ridge at Mag. 4X (Leica binocular), Videos 17, 18 and especially 19 show at mag. 10X (Nikon Eclipse microscope) that the contraction of the nasal area precedes nare invagination. Video 20

shows a magnification of nare ridge invagination at the best possible resolution with our system. It shows that nare opening follows the nasal contraction, and that cells are regularly stacked radially along the nare ridge prior to opening of the nare.

In the videos, especially Videos 17 and 18, we can see an organized tissue structure forming a physical continuity : a sector of tissue is well visible *above* the nasal "placode" in video 17 (dashed lines, arrow in Fig. 7C), and a hairpin of tissue is visible *under* the nasal placode (line and arrowhead in Fig. 7B, dashed line and arrow in Fig. 7C). A furrow is often visible (thin line pointed by arrowhead in Fig. 7B Right, thinner dashed line in Fig. 7C Right, see Video 18). The nasal territory in Fig. 7C, at the moment of nare opening, is similar to the one already present just after neurulation (Fig. 5C, end of Video 10).

During formation of the nasal pit it is seen that cells register ("align" or "stack") along the edge of the presumptive nostril edge or ridge (arrowhead in Fig. 7C from Video 17, and also in Video 19 –not the same embryo). This cell stacking is also visible in the eye and the ear (see Video 20 of ear formation, or Fig.4 in Ref. 4). The nasal pit edge follows a horseshoe shape oriented in the direction of the mouth-eye corner. This horseshoe is actually the top part of the hairpin of tissue visible in the tissue, in the same spirit as the ear is the top part of an otic hairpin of tissue [4].

At the end of all this process, the horseshoe shape of the nostril is quite recognizable (HH20, Fig. 7D), and there is a thin thread running from the nose all the way up to the top of the nasal vesicle. This thread connecting the nostril to the median line makes a shallow furrow separating the ocular and nasal vesicles (Fig. 7D Right).

In summary, the nasal territory is not at all round, it rather has a hair-pin shape from start, a hairpin laying inside a sector. This hairpin shape is deformed by the ballooning of the nasal vesicle, but it is still present at all developmental stages. Returning to Videos 3, 4 and 10Right, we see that the position of this hairpin corresponds to a thin sector located between the presumptive eye sector and the presumptive mouth sector (arrow in Fig. 2B). During mouth contraction the sector bounded by the presumptive mouth and presumptive eye corner is flexed and folded towards the median axis, thus generating a hairpin of tissue located inside a sector (the white hairpin overlaid in Fig. 2B). This sector is also visible in Videos 7, 9, 11 and 22, where it appears as a darker wedge, and especially in Video 10, where the hairpin is quite visible by the end.

Dynamic analysis

In the videos above of nasal pit formation, we observe movements. These can be extracted by Particle Imaging Velocimetry (PIV, see **Supplementary Material PIV**). First, we observe that the brain vesicles dilate (Fig. 8A, from Video 12). Furrows or valleys appear as these vesicles dilate : something linear hinders the dilation. These valleys on the brain vesicles already exist as visible kinks

during neurulation (Videos 2, 4) and they lock the position of the eyes and of the nose. In a late stage embryo, it is common knowledge that these furrows also serve as mechanical cue to position the main blood vessels, as seen classically in a mouse embryo E.13.5 (Supp. Fig. 3). When following in more detail the expansion of the brain vesicles we observe a gradient of movement (i.e. shear) parallel to the furrows with a maximum inside the furrow (Fig. 8B).

During formation of the nasal pit and nares, we repeatedly observe a strong contraction, located between the presumptive nare and the eye (N=10 embryos, 100%). (Fig. 9A, B, C, Videos 15 to 20). When the movement is observed in detail it is seen that there is a movement of the presumptive nasal territory towards the eye-mouth corner. The movement we observe is a contraction of the hairpin (Fig. 10A). The deformation in the hairpin increases during time until there is a relaxation (Fig. 10B). This contraction and relaxation correlates with the sudden appearance of the nostril edge (Videos 15 to 19), the nostril edge forms by contraction of the ridge, which causes invagination and opening of the nares (see carefully Video 20).

Sporadic endogenous contraction twitches are observed in the oculo-nasal area (see Video 23 Fig. 11A) prior to nose morphogenesis. As the period of contraction is a couple of minutes, the rate of frames acquisition must be in the 5 seconds range in order to resolve these contraction movements in detail. These twitches are the manifestation of an excitable behavior, which we have found elsewhere during embryo development [29], especially in the ear sector, which also exhibits sporadic contraction twitches preceding morphogenesis [3]. These sporadic contractions are not just in plane, they flex the ectoderm towards the interior (11B, Left, Video 24), this is also observed at the moment of eye morphogenesis (Fig. 11B Right, Videos 25, 26 shows the flexure triggered by the twitch). When we follow quantitatively by PIV the movement of flexure, both in the nasal area : Fig. 11B Right, and in the eye area : Fig 11B Left, we see that the superficial twitch compresses the underneath tissue (star) and it is followed by a delayed response of the underlying tissue which responds to the ectodermal twitch by its own movement of flexure (arrow).

Discussion

These observations suggest a physical, mechanistic, rationale to nasal pit origin. First of all, the blastodisc is structured in sectors and rings, as reported earlier [3,4]. During neurulation, the chord extends : the boundaries of the sectors forming physical landmarks are stretched posteriorly. Careful observation of the Videos such as Video 2, shows that such landmark lines are present on the blastula surface that they are stretched and that they hinder tissue expansion. This forms the kinks or furrows in the neural tube surface. The ocular territory is locked by such kinks at the boundaries of one sector (Fig. 3). This localizes the outward bulge forming the eye territory during brain dilation. The extension of the eye capsule takes a rotatory start under the convergent-extension movement

[25,26,27] (Fig. 4). The presumptive eye territory swerves between the surface ectoderm and the dilating neural tube (Video 13, Fig. 11A).

Not suprisingly, the anterior sector is quite symmetrical, and it is associated to mouth formation and head flexure (Video 27) as reported before [4]. However, if we look in detail the situation in between the eye sector and the mouth sector, we see that the tissue at the blastula stage (hence a rather 2D layer) undergoes an in-plane flexure or folding movement under both the contraction of the mouth sector and the pull of the chord, which creates a deep kink which is the presumptive hairpin of the future nasal pit, with its own sector connecting it to the median line. Actually, this situation is directly visible in many fish such as the dogfish, as if the dogfish development were arrested earlier than the chicken development (Fig. 1A Middle Left). While in the dogfish, there is an actual furrow between the nares and lips, in the seabream fish the furrow is healed, but a hairpin of tissue connecting the lips to the nares is still very well visible in the adult (Fig. 1A Middle Right, please observe carefully the tissue in between the nare and the upper lip of this fish.)

We have observed that during neurulation, closure of the notopore, likely by preventing fluid escape, causes or at least contributes to cause the strong dilation of the brain vesicles. The dilation of the vesicle, the continued contraction of the mouth area, and the pull along the nasal sector hardly deforms the nasal area which remains a horseshoe at the apex of a U-turn or hairpin of tissue. This is how the nasal pit territory forms ; Fig. 12 A summarizes schematically the process. These geometrical facts explain readily why the placode is not circular, and why it is a horseshoe inserted midway inside a sector. Also, if nose formation occurs earlier during the morphogenetic movements, the oculo-nasal area will be morphologically different : at early stages it will look for example as the dogfish olfactory system. Early stages of chicken development are reminiscent of what is seen in fish. If the furrow of the hairpin does not heal, a nose-to-mouth slit will be apparent.

The tension in the strings or cables (the radial lines or rays seen inside the blastula) explains readily the presence of the valleys separating the brain vesicles (Fig. 12B). Indeed, a linear tension T**t** along a curved line with tangent vector **t** , imparts an inwards force T**n**/R by Laplace formula, in which **n** is the normal vector; this is the force which hinders the ballooning of the vesicles. This inwards force is equilibrated by the inverted curvature in the direction perpendicular to the valley direction (Fig. 12B top Right). Now, in addition, we also observed in Fig. 8 a linear force along the furrow generating a shear force. This linear force is what would be expected for a non-uniform tension, with a gradient. Indeed, a gradient of linear tension generates an in-plane force $\partial_s \mathbf{T}(s) = \partial_s T(s)\mathbf{t}$ along the curvilinear direction (Fg. 12B Bottom). It has been shown in Ref. 17 that the early embryonic movements proceed by a gradient of tension which generates dipolar and quadrupolar movements. Such a gradient of tension generates a force which orients visco-elastic movements towards the

corner of the mouth. This is why, as the mouth territory constricts, both the nasal area and the eye area point and converge in that direction. Therefore, we find a common explanation to the localization of the nasal pit, its form, its orientation, its correlation with mouth and eye formation, and the presence of long-ranged valleys occupied by tissue cables and defining the brain vesicles. Of course, depending on the magnitude of the forces, the pattern of convergence of the nose the eyes and mouth, encapsulated in the shape of the nasogenian groove, will be more or less acute.

The spurious contraction twitches and the deeper contractions which follow the surface contractions show that the tissue is contractile and active, that the contractility is latent and excitable, and that the spatial pattern of the contraction is congruent with the geometry. This excitability or latent contractility provides also a mechanism explaining why some culture media are able to trigger rapid nasal pit formation [30], since contractions are sensitive to ionic concentrations, and ATP levels. In the same spirit, we have shown in Ref. 29 that, during limb development, embryonic tissue contraction has a pattern which follows tissue geometry. Here the hairpin of tissue contracts following the existing prepattern, in a similar fashion as peristaltic waves along the lung [31] or the gut [32]. The propagation of the contraction along the nasal hairpin triggers the formation of the nose by contraction of the edge of the hairpin.

One important aspect of the mechanism of ectoderm delamination and buckling lies in the fact that the excitability is not just in plane but also out-of-plane. As shown in Videos 24,25,26, the twitches propagate in depth and stimulate contraction of the underneath cell layers. In plane, the tissue is close to continuous, but it is discrete out of plane (there exist stratified cell layers). Since the tissue layers are triggered in a discrete sequence, the propagation from one layer to the next happens in sequence, with some discrete delay. This causes a strain mismatch between layers (one layer starts to constrict, while the other is already relaxing), thus favoring delamination and roll-up of the nare ridge (delamination inside the nare area is manifested by a double nare edge shortly visible in Video 20). Since, in addition, there is a sector of tissue stretched anisotropically in the oral to dorsal direction, delamination and invagination occurs sooner in the top part of the horseshoe forming the initial nasal pit cavity, as observed.

The observations reported here explain also in a straightforward manner why there exists a lacrimal canal between the eye and the nose. The canal connects the nares to the U-turn fold of the eye cupula (the fornix), because they correspond remotely to neighbouring areas in the corner of the mouth (Fig. 2B, see also Video 9), and they are both dragged towards each-other by tissue contraction in the corner of the mouth area.

The taxonomy shows the interesting case of the lampreys, and other jawless fish. The agnatha have one single nostril, along the median axis (Fig. 1B Top), in between the eyes [8,9,20]. It appears that the single nostril of the lamprey is in fact the semi-hole formed by the U-turn or median

fornix at the apex of the neural tube (anterior notopore), visible for example in our Video 22 in frontal view, or in Fig. 6A, Top Left. This shows that U-turn fornices such as the eye fornix or the notopore are favorable spots for organ development, being an almost closed hollow niche. In most vertebrates this area locks the pituitary gland [20].

One may wonder why there is a bifurcation between a single nostril along the median axis, or two on either sides, and whether this is a mere evolutionary coincidence happening by hazard, or a true morphogenetic bifurcation. Systems biology would invoke some induction loop selected at random. Physics would rather search for a driving parameter causing some bifurcation. We have observed that closure of the notopore (nasal pit in the lamprey) enhances brain dilation. We also observed that there is a tension force in the furrows oriented rostrally. We see that if the rostral force in the threads or cables is increased, the head rocks forward more (as in Video 27). Increasing the linear tension along the median axis pulls on the notopore; then the notopore is stretched in a direction which increases the likelihood of notopore closure (the median force being increased, the neural folds tend to close more tightly, as when pulling on a rubber foil, see Fig. 3B in Ref. 4), but conversely, the increased pull in the cables is associated to an increased pull forming a more pronounced hairpin which favors the formation of paired nostrils. This comes from the fact that, while out-of-plane buckling is enhanced by traction, in plane deformation is enhanced too. Hence, there is a dynamic rationale to the transition from agnatha (no jaw, one single nostril), to gnathostomes (a jaw and paired nostrils), by increase of the linear force in the cables (a one dimensional parameter acting simultaneously on head flexure and nostril prepatterning).

Moreover, if we return to the picture of the thornback ray (Fig. 1B Bottom) we see that the four nares are actually associated to the convex side and the concave side of the nasal sector, deformed in a hairpin manner, each side of the fold corresponding to an almost closed niche.

While all these movements may seem awfully complex and beyond any mathematical analysis, a parsimonious physical picture can nevertheless be given (Fig. 12C, Video 28). The presumptive nasal territory finds itself at the oral boundary (represented by the black line). The contraction of the DV boundary advects visco-elastically the entire tissue. In a very crude approximation, we assume a contraction force along the oral boundary [3,4], modelled by a force term aligned at the D-V boundary (red arrows). By flow conservation, it is equivalent to assume a contraction along the D-V boundary or to assume a traction at right angle, along the nasal sector (this, by the way, constrains the developmental process). If we assume a symmetrical contraction, we find generic deformations as in Fig. 12C (Top). But since the nasal territory is not along the median axis, we may introduce an asymmetry of the quadrupolar flow with a gradient of contraction oriented towards the median axis, specified by two dipolar forces one of higher manitude along the median axis. Thus, we find typical generic deformations as in Fig. 12C (Bottom). In all cases, we find

horseshoe shapes oriented towards the oral line, with a secondary lateral concavity corresponding to the second nare in fish with four nares.

Conclusion

This works shows that face dynamics in the chordate phylum is not at all arbitrary. It is prepatterned by a set of contracting lines forming rings and sectors. These rings and sectors are related to the early pattern of zygote cleavage [3,4]. The dynamics of morphogenesis is actually latent in the geometry of cell division, which is biaxial (the sequence of cell cleavages occurs at right angles). There is a strong coupling between geometry and dynamics, both in-plane and out-of-plane. Cells tend to align in the existing pattern, under in-plane traction forces and form cables. The lines of the pattern behave as tiny pulling strings. In the first place, cell cleavage occurs by contractions, which prepattern this set of strings.

We have shown that in the early embryo, the contraction of the tissue is both in-plane and out-of-plane. The out-of-plane component of the contractions creates out-of-phase strains which favor delamination in a stratified biological tissue. All this renders animal body formation, with its sensory organs, a robust dynamical process explaining the generic features of vertebrates face, and the fact that sensory organs are connected to the brain. In the specific case of the nose, the pattern cannot be reduced to a round placode; there is a holistic aspect to nose formation, with simultaneously a canal towards the eye, a slit towards the mouth, and a likely physical bifurcation related to force actuation, all related to the dynamics of contraction in a pattern of radial and orthoradial lines. Along these lines, contraction forces are long ranged and they induce holistic features such as grooves or furrows which are readily observable on any face. The molecular cause of these contractions is likely to be the actin-myosin complex, which causes contraction of rings at early embryonic stages [34, 35]. More generally, the lines present in the early blastula serve as mechanical cues for the entire morphogenetic process, and they connect the sensory organs to the inside of the brain. The dynamics explained here may help to clarify certain teratologies such as holoprosencephaly [6]. These face teratologies show a continuous spectrum of abnormalities, ranging from almost normal face with a mild narrowing of the inter-ocular distance, to a very narrow front with cyclopia, and absence of nose. It makes sense that, since the initial morphogenetic movements comprise a contraction of the oculo-naso-oral area along a circular line running around the Dorso-Ventral boundary and connecting the mouth, the nares, the eyes and even the ears, a smaller or larger traction force along such a line will lead *in fine* to faces with eyes and nares more or less asunder.

Ethics statement : All experiments reported here are authorized by french rural law, articles R214-87 to R214-137, which authorize experiments on embryonic forms of ovipars until hatching.

Data Availability Statement. All the data, mostly high definition Time-Lapse Videos of development, are freely available upon request by the author. The custom Java plugins for tissue tracking, and strain tensor analysis are freely available upon request.

Acknowledgements : I dedicate this article to the memory of late French physicist Yves Couder (1941-2019), who used to say that the dynamics of morphogenesis is to be looked for in the geometry. I acknowledge the financial support of the master BioMedical Engineering of Université de Paris Cité, of the generous donators of the Fondation CNRS and of the SATT ERGANEO. I acknowledge the friendly support of Amanda Brun, Nicolas Chevalier, Florence Gazeau and Hugo Salmon. I am grateful to anonymous reviewers for constructive remarks.

References

1. A. Graham & S. M. Shimeld, The origin and evolution of the ectodermal placodes, *J. Anat.* **222** (1), 32-40 (2013). doi: 10.1111/j.1469-7580.2012.01506.x. Epub 2012 Apr 18.

2. R. Horie, A. Hazbun, K. Chen, K. *et al.* Shared evolutionary origin of vertebrate neural crest and cranial placodes, *Nature* **560,** 228–232 (2018). https://doi.org/10.1038/s41586-018-0385-7

3. V. Fleury, A. Abourachid, A. Peaucelle and O. Plateau, Second order division in sectors as a prepattern for sensory organs in vertebrate development, *Theory in Biosciences*, Special Issue Geometries and phenomenology of the Living (2021). https://doi.org/10.1007/s12064-021-00350-w

4. V. Fleury, A. Abourachid, A biaxial tensional model for early vertebrate morphogenesis, *Eu. Phys. J. E* **45**, 31 (2022). https://doi.org/10.1140/epje/s10189-022-00184-4

5. D. R. Lefevre & S. K. Freitag, Update on imaging of the lacrimal drainage system, *Semin. Ophthalmo.l* **27** (5-6), 175-86 (2012). doi: 10.3109/08820538.2012.711413.

6. C. Dubourg, C. Bendavid, L. Pasquier, C. Henry, S. Odent , V. David, Holoprosencephaly, *J. Rare Dis.* **2** (8) (2007).

7. N.-C. Liu, E. Troconis, L. Kalmár, D. Price, H. Wright, V. Adams, D. Sargan, J. Ladlow, Conformational risk factors of brachycephalic obstructive airway syndrome (BOAS) in pugs, French bulldogs, and bulldogs, *PLoS ONE* **12** (2017): e0181928. https://doi.org/10.1371/journal.pone.0181928

8. J. P. L. Cox, Hydrodynamic aspects of fish olfaction, *J. R. Soc. Interface* **5** (23), 575–593 (2008).

9. Z. Gai & M. Zhu,The origin of the vertebrate jaw: Intersection between developmental biology-based model and fossil evidence, *Chinese Science Bull.* **57** (31) (2012).

10. I. Schwab, The evolution of eyes: major steps. The Keeler lecture 2017: centenary of Keeler Ltd. *Eye* **32**, 302–313 (2018). https://doi.org/10.1038/eye.2017.226

11. J. B. Miesfeld, N. L. Brown, Eye Organogenesis : A hierarchical view of ocular development, *Curr. Top Dev. Biol.* **132**, 351-393 (2019). doi: 10.1016/bs.ctdb.2018.12.008

12. R. K. Ladher, Changing shape and shaping change: Inducing the inner ear, *Semin. Cell Dev. Biol.* **65**, 39-46 (2017). doi: 10.1016/j.semcdb.2016.10.006

13. X. Sa, K. Raj, R. K. Ladher, Early steps in inner ear development: induction and morphogenesis of the otic placode, *Front. Pharmacol.* **6**, 19 (2015). doi: 10.3389/fphar.2015.00019.

14. B. Van Valkenburgh, T. D. Smith, B. A. Craven, Tour of a Labyrinth: Exploring the Vertebrate Nose, *The Anatomical Record* **297**, 1975-1984 (2014).

15. K. E. Whitlock, A new model for olfactory placode development, *Brain Behaviour and Evolution* **64** (3):126-40 (2004). doi: 10.1159/000079742.

16. S. Gilbert, *Developmental Biology*, (Sunderland Ma. Sinauer, 1997).

17. V. Fleury, Clarifying tetrapod embryogenesis by a dorso-ventral analysis of the tissue flows during early stages of chicken development, *Biosystems*, Special issue "Morphogenesis", **109**, 460-474 (2012).

18. V. Fleury, V. A. Murukutla, N. Chevalier, B. Gallois, M. Capellazzi-Resta, P. Picquet, A. Peaucelle, Physics of Amniote formation, *Phys. Rev. E* **94**, 022426-022444 (2016).

19. V. Hamburger, H. L. Hamilton, A series of normal stages in the development of the chick embryo, *Journal of Morphology* **88** (1), 49–92 (1951).

20. K. Ushida, Y. Murakami, S. Kuraku, S. Hirano, and S. Kuratani, Development of the Adenohypophysis in the Lamprey: Evolution of Epigenetic Patterning Programs in Organogenesis, *J. Exp. Zool. (Mol. Dev. Evol.)* **300B**, 2-47 (2003).

21. D. W. Thompson, *On Growth and Form* (Cambridge University Press Cambridge 1917).

22. M. J. Cohn, J. C. Izpisua-Belmonte, H. Abud, J. Heath, Ch. Tickle, Fibroblast Growth Factors Induce Additional Limb Development from the Flank of Chick Embryos, *Cell* **80**, 739-746 (1995).

23. M. Levine, Molecular bioelectricity: how endogenous voltage potentials control cell behavior and instruct pattern regulation in vivo, *Mol. Biol. Cell* **25** (24), 835-850 (2014).

24. V. Fleury, N. Chevalier, F. Furfaro, and J.-L. Duband, *Eu. Phys. J. E* **38**, (6) (2015).

25. R. Keller, Shaping the Vertebrate Body Plan by Polarized Embryonic Cell Movements, *Science* **298**, (5600), 1950-1954 (2002). doi: 10.1126/science.1079478.17.

26. M. Tada, and C.-P. Heisenberg, Convergent extension: using collective cell migration and cell intercalation to shape embryos*, Development* **139** (21), 3897–3904 (2012).

27. V. Fleury, A change in boundary conditions induces a discontinuity of tissue flow in chicken embryos and the formation of the cephalic fold, *Eu. Phys.Lett.* **34**, 73-86 (2011).

28. J. R. Martinez-Morales, F. Cavodeassi, P. Bovolenta, Coordinated Morphogenetic Mechanisms Shape the Vertebrate Eye, *Front Neurosci.* **20** (11), 721-729 (2017). doi: 10.3389/fnins.2017.00721.

29. V. Fleury, V. A. Murukutla, Electrical stimulation of developmental forces reveals the mechanism of limb formation in the chicken embryo, *Eu. Phys. J. E.* **42**, 104 (2019) doi:10.1140/epje/i2019-11869-8.

30. M. S. Smuts, Rapid nasal pit formation in mouse embryos stimulated by ATP-containing medium, *J. Exp. Biol.* **216** (3), 409-414, (1981).

31. K. K. Bokka, E. C. Jesudason, O. A. Lozoya, F. Guilak, D. Warburton, S. R. Lubkin, Morphogenetic Implications of Peristalsis-Driven Fluid Flow in the Embryonic Lung, *PLoS ONE* **10** (7)**,** (2005): e0132015. https://doi.org/10.1371/journal.pone.0132015**.**

32. N. R. Chevalier, N. Dacher, C. Jacques, L. Langlois, C. Guedj, O. Faklaris, Embryogenesis of the Peristaltic Reflex, insights into the myogenic to neurogenic transition of gut motility, *Journal of Physiology* **597** (10) 2785-2801 (2019).

33. E. Rozbicki, M. Chuai, A. I. Karjalainen, F. Song, H. M. Sang, R. Martin, H. J. Knolker, M. P. MacDonald, C. J. Weijer, Myosin-II-mediated cell shape changes and cell intercalation contribute to primitive streak formation, *Nat. Cell Biol.* **17**, 397-408 (2015).

34. C. F. MacMannus, N. E. Tipping and D. J. Wilson, *Wound Repair and Regeneration* **14**, (1), 61-65 (2004).

35. A. R. J. Westerweel, *Particle Imaging Velocimetry* (Cambridge University Press, Cambridge 2011).

FIGURE and CAPTIONS

Figure 1A

Figure 1B

Figure 1B

Figure 1. 1A Examples of nostrils. Most animals have paired nostrils. Generally the holes present a horseshoe shape, as in sharks (Top Left). There also generally exists a groove (stingray Top-Right) or some visible line between the nostril and the mouth (seabream, Middle Right). Quite often there are slits running between the nares and the mouth (stingray, Top Right), or from the nare towards the eye (naso-lacrymal canal as in dogs, Bottom Right). Humans have a nasogenian groove (arrow in Paulette Goddard, Bottom Left). There exists a secondary groove below the eyes, more visible in elderlies. **Figure 1B Different nostrils shapes.** Not all animals have paired nostrils. Agnatha such as the lamprey (Fig. 1B Top) have a single nostril on top of the head, along the median axis. Thornback stingrays (Fig. 1B Bottom) and many other fish have paired incurrent and excurrent nostrils forming a complex of four nostrils.

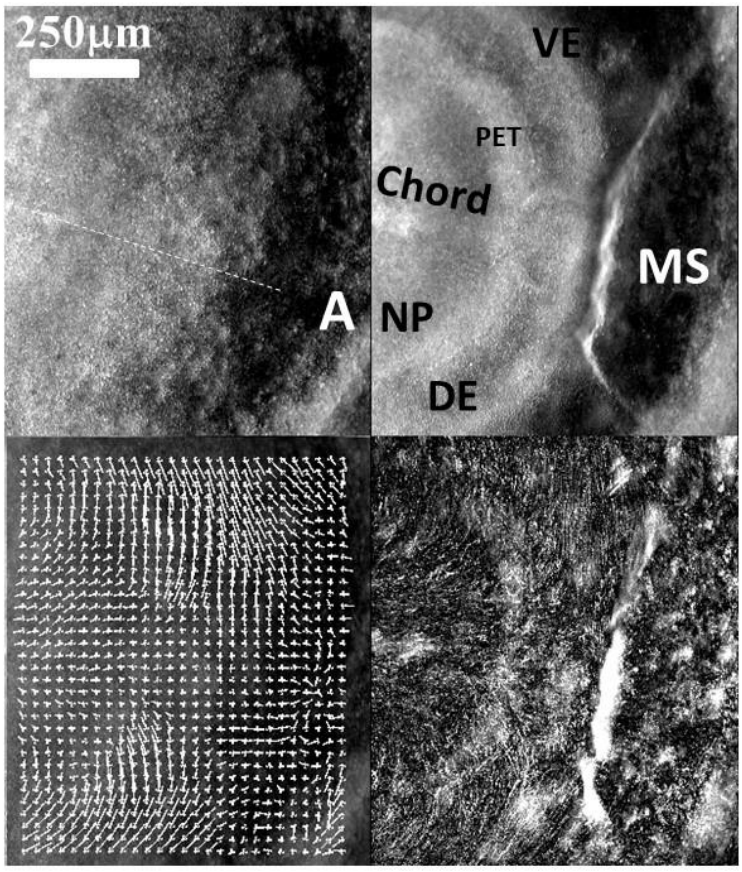
250μm
A
VE
PET
Chord
MS
NP
DE

Figure 2A

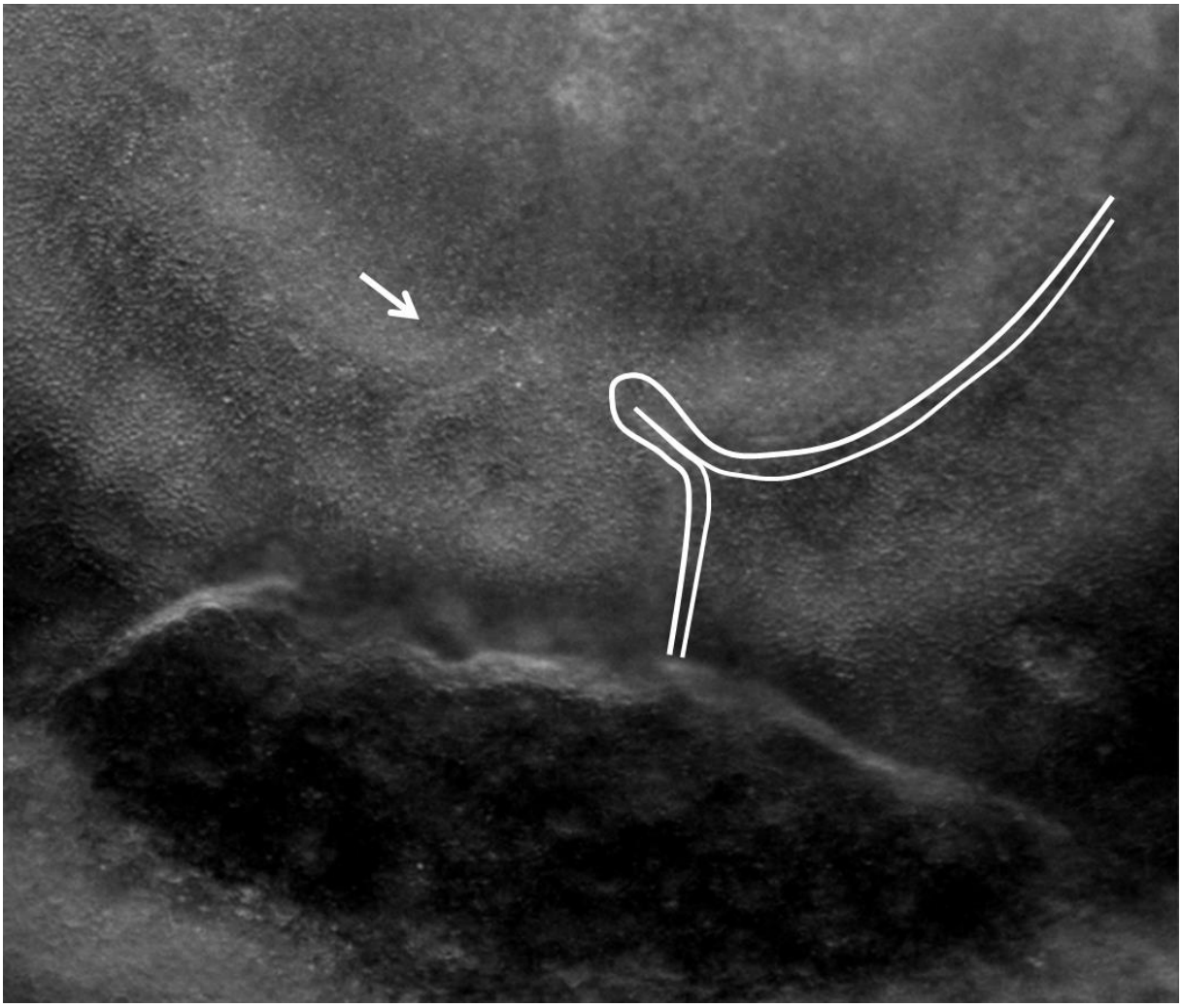

Figure 2B

Figure 2 Fig.2A Initial movements of the blastodisc (see Video 3). The chicken blastula (or blastodisc), exhibits a structure in rings and sectors. The dashed line ending at "A" shows the direction of the Antero-Posterior axis. The lines in ring and sectors of the blastula pattern become more visible during embryogenesis movements (Top Right). The lines sharpen as the embryo constricts and folds along these lines. The internal discoidal plate, visible in the Top Right photo of the panel corresponds to the neural territory or neural plate (NP) ; one finds next the dorsal ectoderm (DE), the ventral ectoderm (VE) and the extra-embryonic organs. The foremost sector, visible here in the Top Right image by two sharp radiating lines, is associated to the mouth sector (MS). The sectors constrict, and during constriction the sectors round off to form, here, the mouth stomodeum (presumptive mouth territory). The Top Left photo shows the starting situation. The Bottom Left shows the PIV map with the movements of the tissue, extracted from Video 3. The Bottom-Right image shows the actual streamlines as obtained by superimposing 30 minutes of images (after background inhomogeneity correction and thresholding). NP: Neural Plate, MS : Mouth Sector, PET: Presumptive Eye Territory, DE: Dorsal Ectoderm. **Fig.2B Presence of a thin sector deformed in a hairpin pattern** During the contraction of the mouth sector one evidences a thin sector at the ocular/oral boundary which is dragged towards the median axis and forms a hairpin.

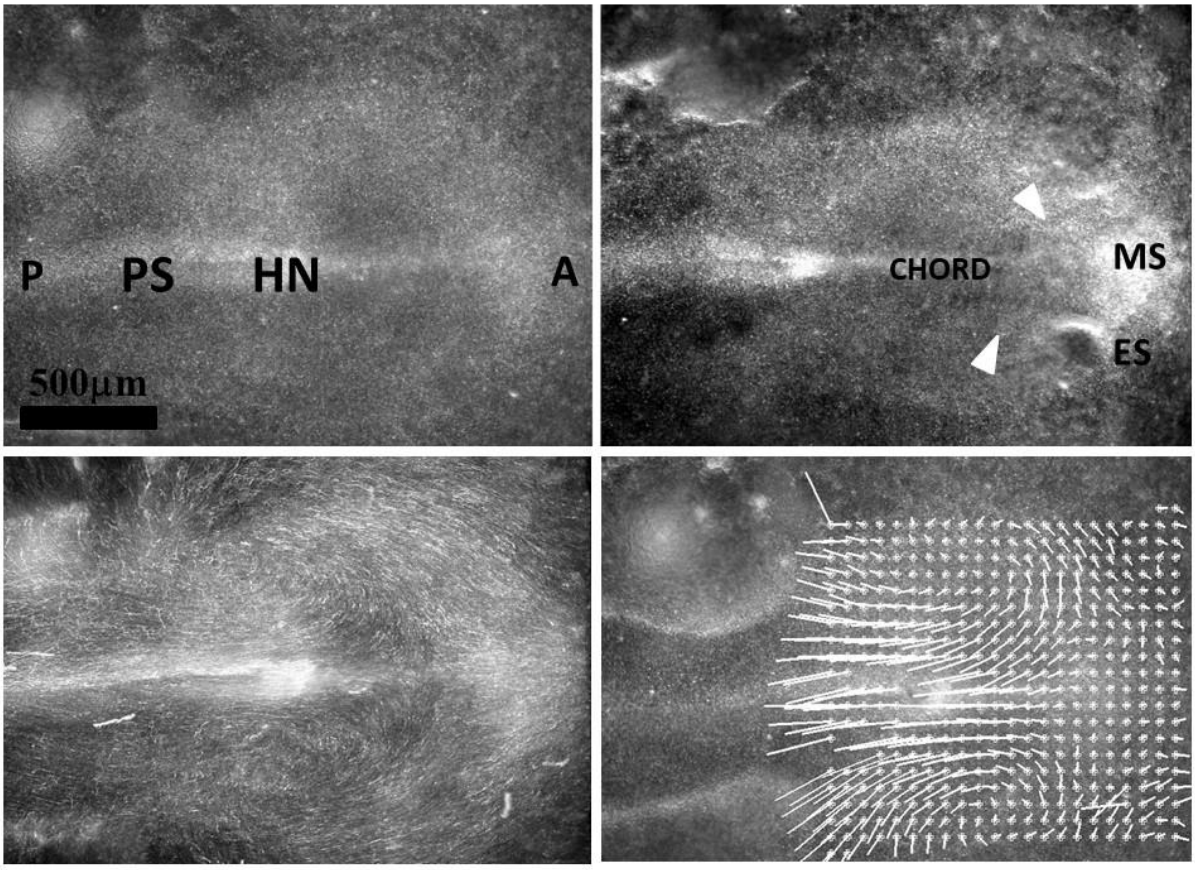

Figure 3A

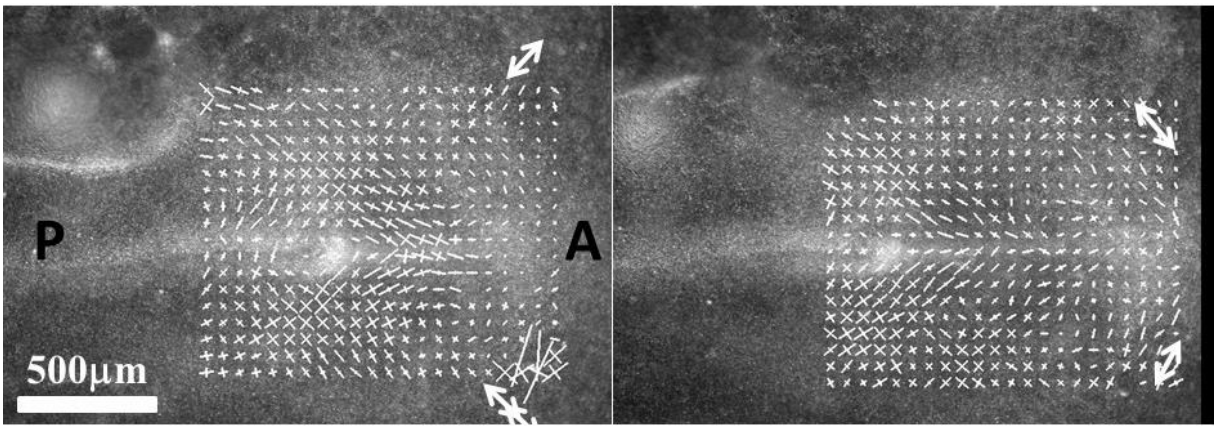

Figure 3B

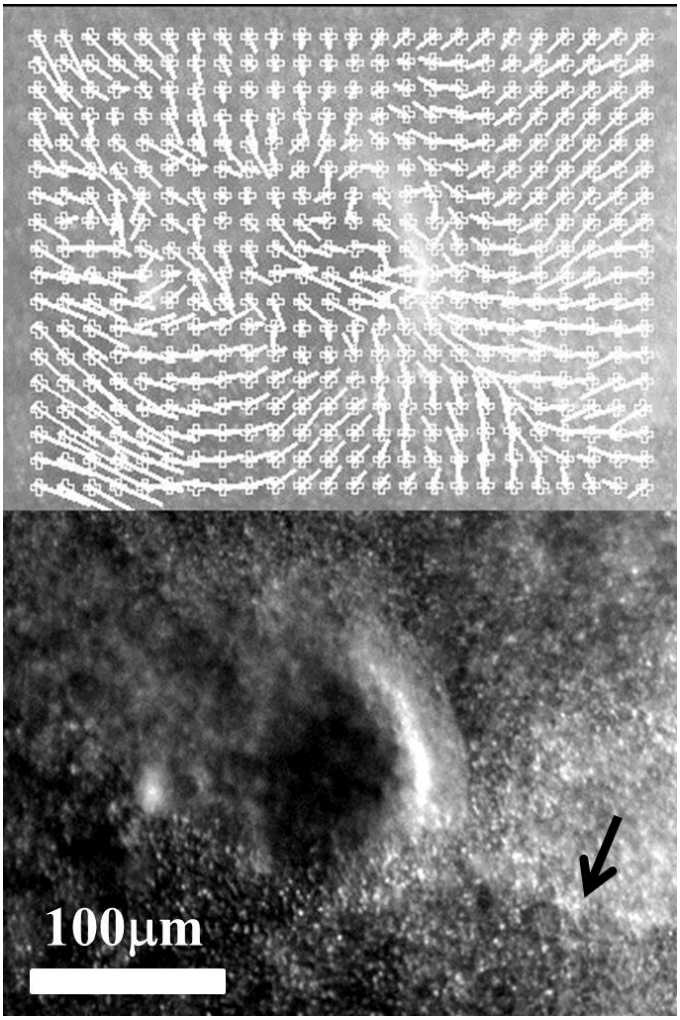

Figure 3C

Figure 3. Early stages of eye placode formation. Fig. 3A The Top-Left photo shows the blastodisc at start of embryo morphogenesis (approx. 20hrs of development, late primitive-streak stage). A stands for Anterior, P for Posterior. At that stage, the avian blastodisc is flat (hence its name). **Fig. 3A** Top-Right shows the blastodisc at the onset of neural roll-up (see Video 4). Elongated sectors corresponding to nasal and ocular territories are visible (white arrowheads). Since the blastodisc is almost flat, we can extract movements and deformations by Particle Imaging Velocimetry (PIV see Supp. Mat. PIV). We first extract the displacement field during the phase of posterior stretch by the chord. The flow map shows a vortical pattern due to the dipolar pull (Fig. 3A Top Right). Fig. 3A Bottom Left shows the superimposition of 1hr of movement, revealing the actual streamlines. **Fig. 3B** Extraction of the strain field at an early stage (+2hr with respect to Fig. 3ATop Left) shows a tensile strain with principle axis oriented in the direction of the sector of the presumptive nasal area (arrow), at the corner of the mouth sector (Fig. 3B Left). In this figure the lengths of the segments are proportional to the eigenvalues of the principal strain tensor (the principal extensions). An eigenvalue of 1 corresponds to ¾ of the grid spacing. At a later stage (+5hr with respect to Fig. 3ATop Left) the anterior sector constricts and neurulation starts, around this moment, the principle strain tensor becomes oriented orthoradially (arrow). This shows that sources of stress have principle axis

at right angles, and they are exerted in cascade: anterior contraction follows posterior traction. **Fig. 3C.** Magnification of the eye placode at the onset of neurulation shows a domain, horseshoe shaped, which is one part of a sector of the blastula. This domain constricts along the D-V boundary, with a rotatory movement oriented towards the inside of the placode. The black arrow points to the Dorso-Ventral boundary.

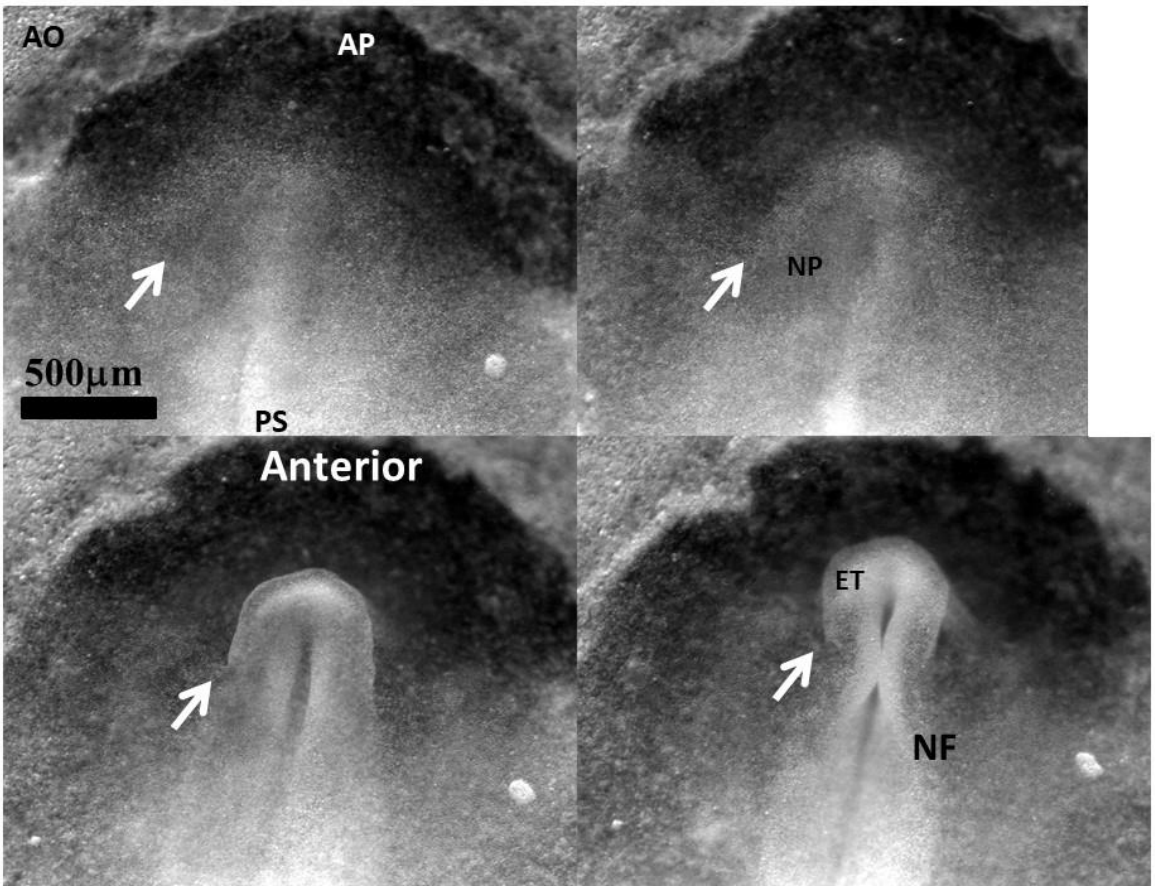

Figure 4A

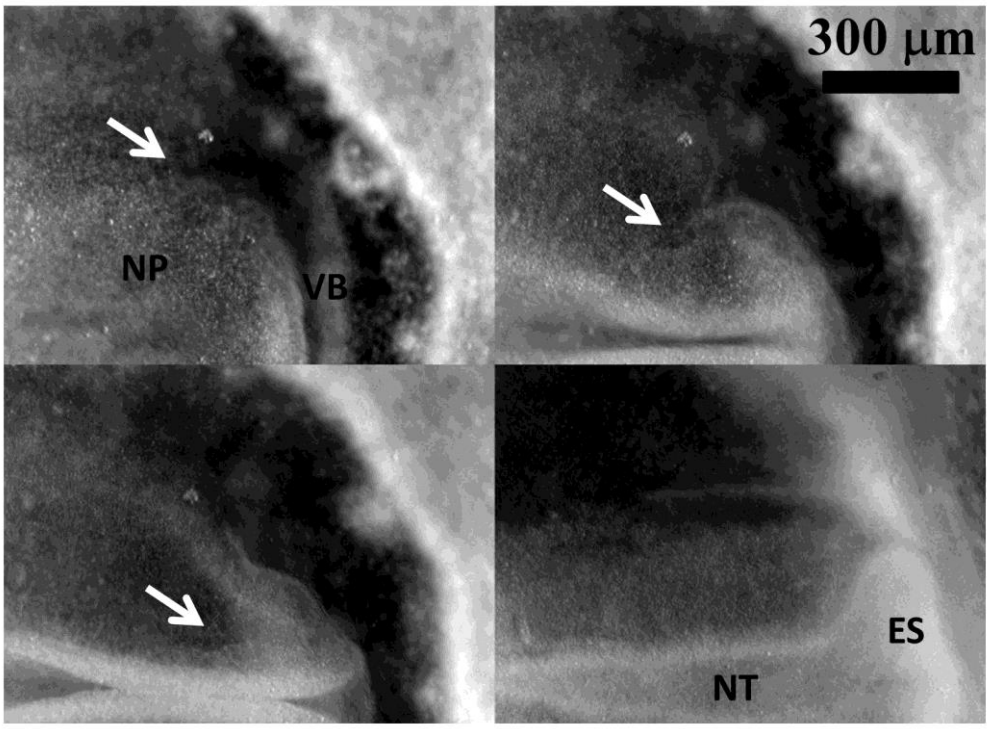

Figure 4B

Figure 4. Early stage of eye formation. Fig. 4A (from Video 5) shows the deformation during early stages of neurulation. The neural territory buckles and forms a first bump locked at the boundary of the sector corresponding to the presumptive eye territory (arrows). **Fig 4B** (from Video 6) The eye stalk starts to expand sideways exactly in front of the bump in the neural folds, locked by the boundary of the sector (arrows). PS : Primitive Streak ; ET : Eye territory ; AP Area Pellucida; AO : Area Opaca ; NT : Neural Tube ; NP : Neural Plate ; NF : Neural Folds; ES : Eye Stalk ; VB : Ventral Boundary.

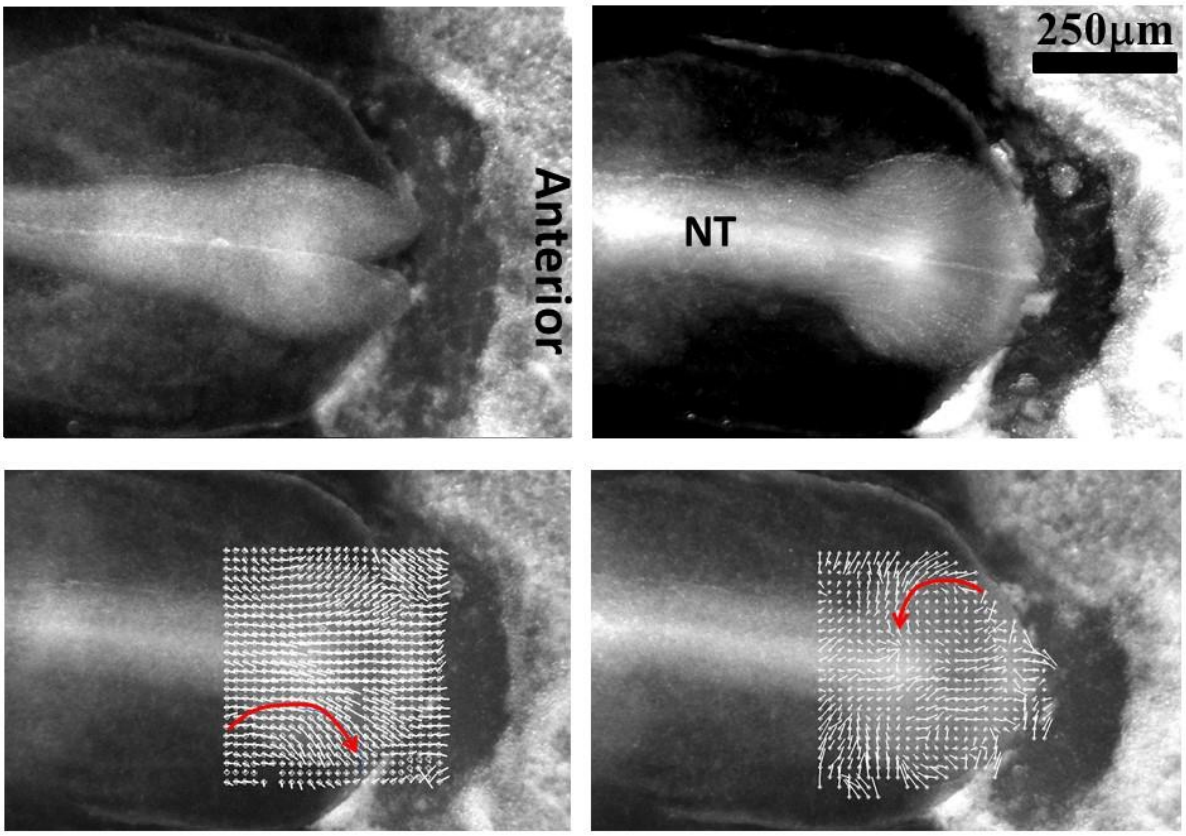

Figure 5A

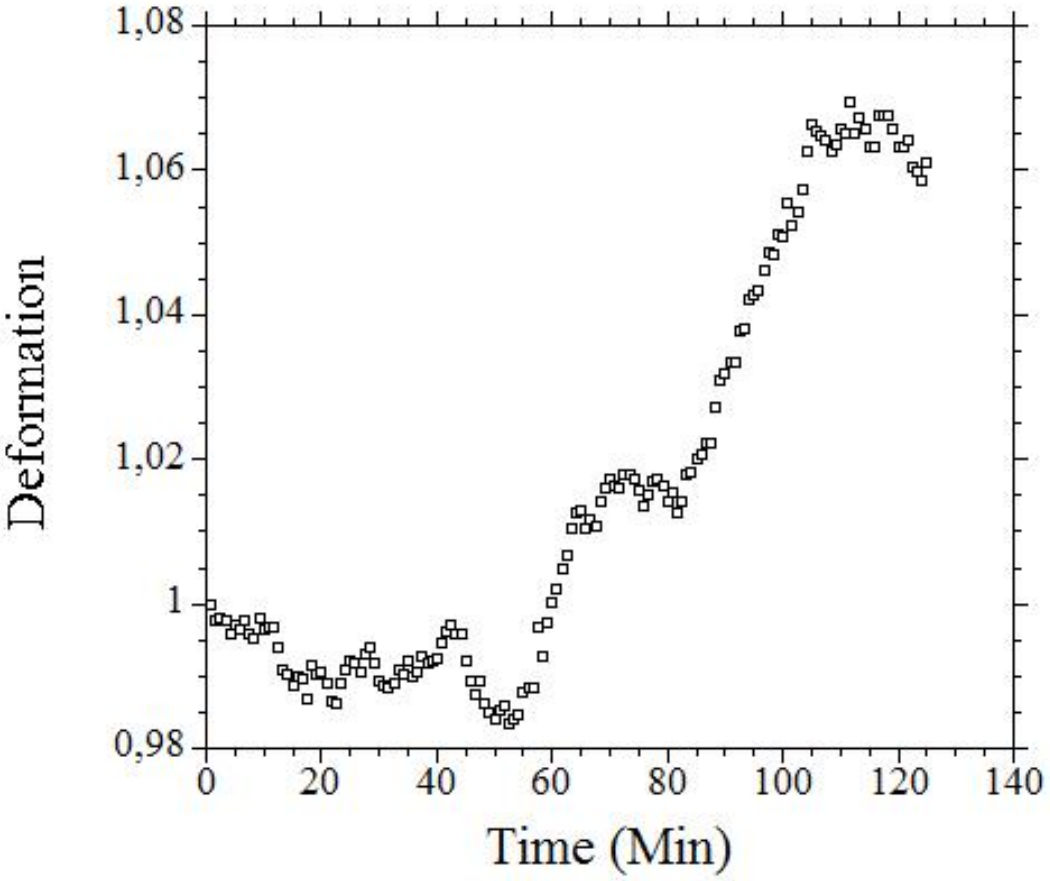
Deformation
1,08
1,06
1,04
1,02
1
0,98
0
20
40
60
80
100
120
140
Time (Min)

Figure 5B

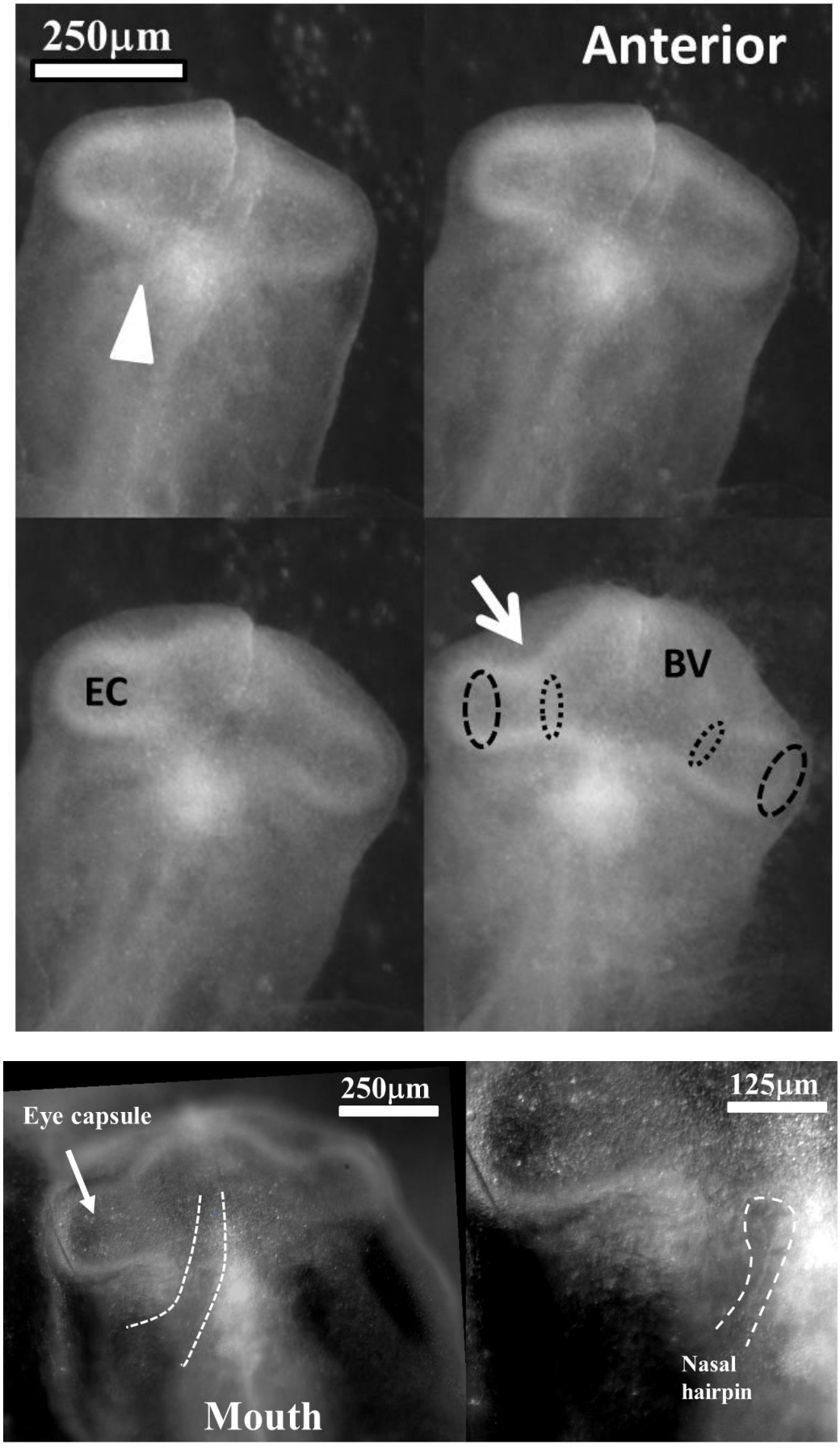
250µm
Anterior
EC
BV
250µm
Eye capsule
Mouth
125µm
Nasal
hairpin

Figure 5C

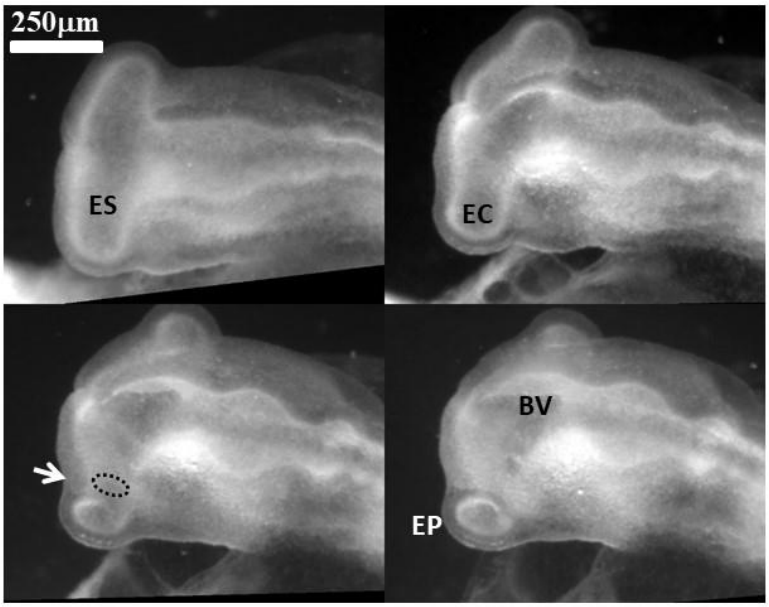

Figure 5D

Figure 5 Physical winding of the eye territory during neurulation Fig. 5A (from Video 7). By the end of neurulation the neural tube (NT) closes. The extension of the tube causes a forward movement and rotatory recirculation of the eye tissue which undergoes a bilateral dipolar tissue flow (red arrow). The dipolar flow orients the eye stalk expansion in a lateral direction. The movement becomes more posterior as the tissue winds. Top-Left the neural tube just before closure. Top-Right : superimposition of frames during 2 hours of movement show the actual streamlines winding laterally. Bottom Left extraction of speeds by PIV just after closure of the tube shows the lateral movement. Bottom Right, two hours later, the movement is more rotatory (arrow) as a consequence of physical winding of the tissue. **Fig. 5B.** The closure of the neural tube correlates with a sudden dilation of the brain vesicle and of the oculo-nasal territory, and even of the entire head, and to an acceleration of the eye extension (see Videos 9, 10 and 11 in which the acceleration of brain dilation is quite visible). The graph shows the deformation rate between the presumptive eye and nose

territory, before and after notopore closure extracted from Video 9 (4 frames of which in Fig. 5C). **Fig. 5C**. Fig. 5C Top (from Video 9) : Early stage of eye stalk extension, as seen from underneath at Mag. 4X, shows the constriction of the basis of the stalk as it expands (arrow); also, the nasal sector is visible (arrowhead). After posterior winding of the eye capsule, the eye placode will correspond to the ectoderm facing the eye capsule (large dots line). BV: Brain vesicle, EC: Eye capsule. Fig. 5C Bottom (from Video 10): At Mag. 5X and 10X, the formation of the nasal hairpin, in between the eye and mouth territories, is visible. The nasal hairpin forms a loop, the center of which will define the nasal placode and pit. **Fig. 5D** (from Video 12). A ¾ dorsal view of eye stalk expansion shows the flattening of the eye stalk against the dorsal ectoderm, and the progressive constriction of the eye stalk (arrow). The flattening against the ectoderm forms the round ocular placode. ES : Eye Stalk, EP : Eye Placode, BV : Brain vesicle.

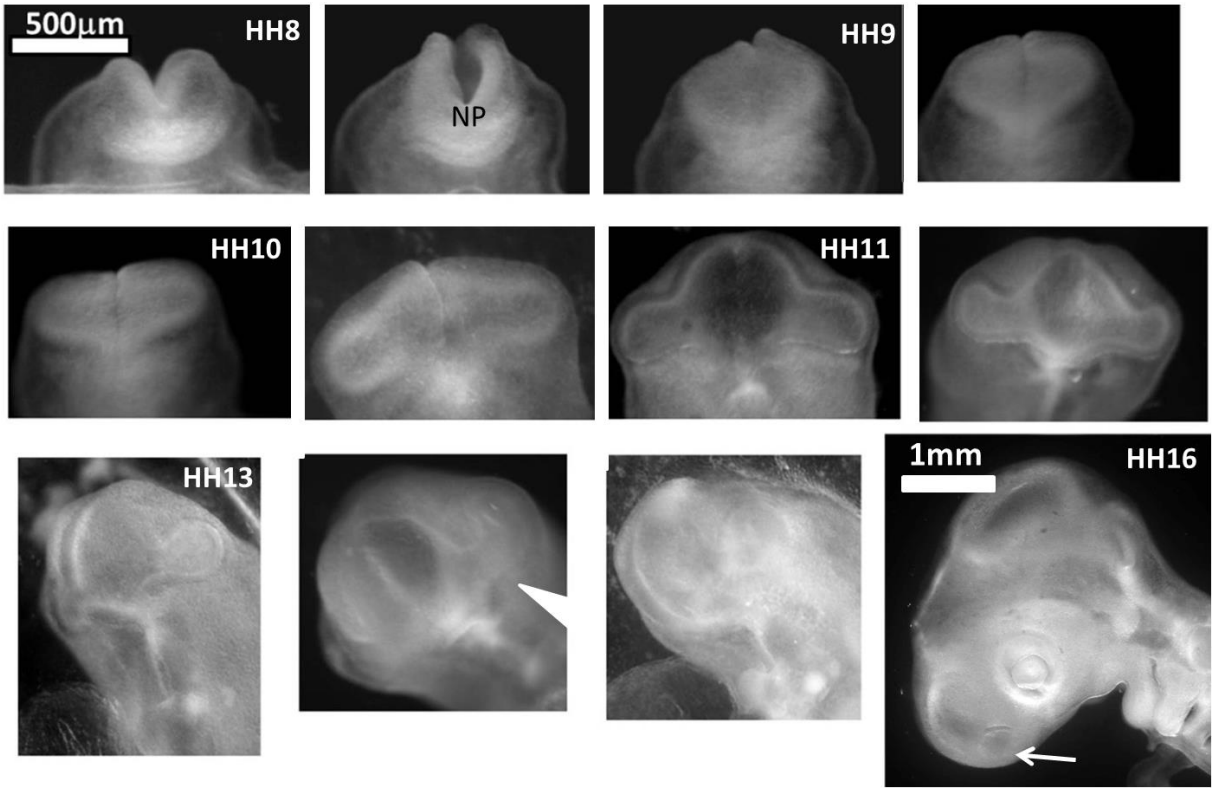

Figure 6 A

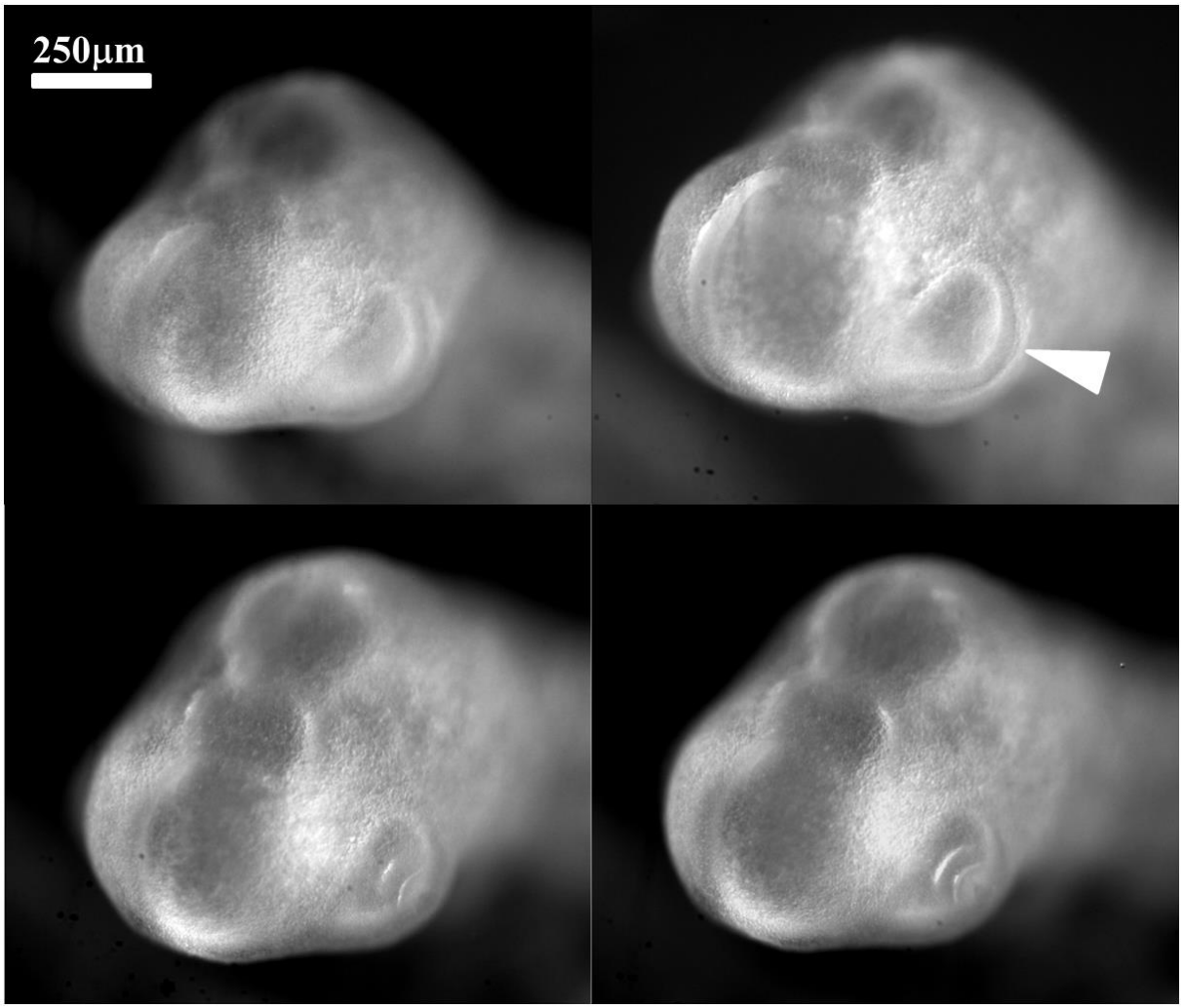

Figure 6B

Figure 6 Formation of the eye. Fig. 6A Table of images of head stages since neurulation and until nose pit formation. One observes a winding of the eye stalk oriented in the posterior direction such that the root or basis of the eye stalk (the orifice opposite to the eye territory, located at the other end of the eye stalk tunnel and opening into the brain vesicle) becomes offset from the eye capsule (arrowhead). The so-called eye placode is the result of the flattening of the eye capsule against the surface ectoderm. In the last image the arrow points to the nasal pit. A sector of tissue with different contrast is also visible between the nasal pit and the median axis (NP : Notopore). **Fig. 6B** A ¾ facial view shows the ocular placode (arrowhead). The placode has an oblate form with an asymmetry. The eye territory points towards the oral and nasal territories. (Montage obtained from the time-lapse of eye formation in Video 14).

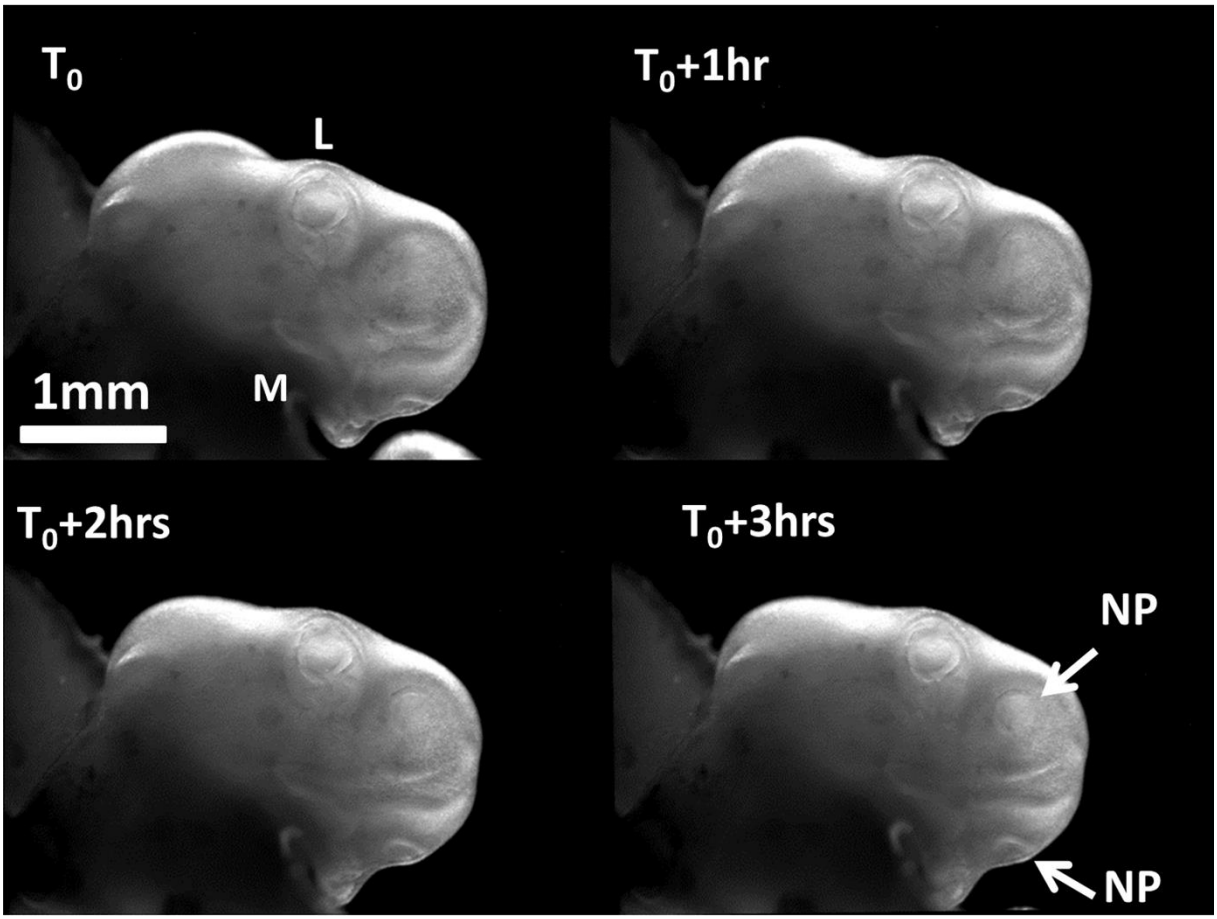

Figure 7A

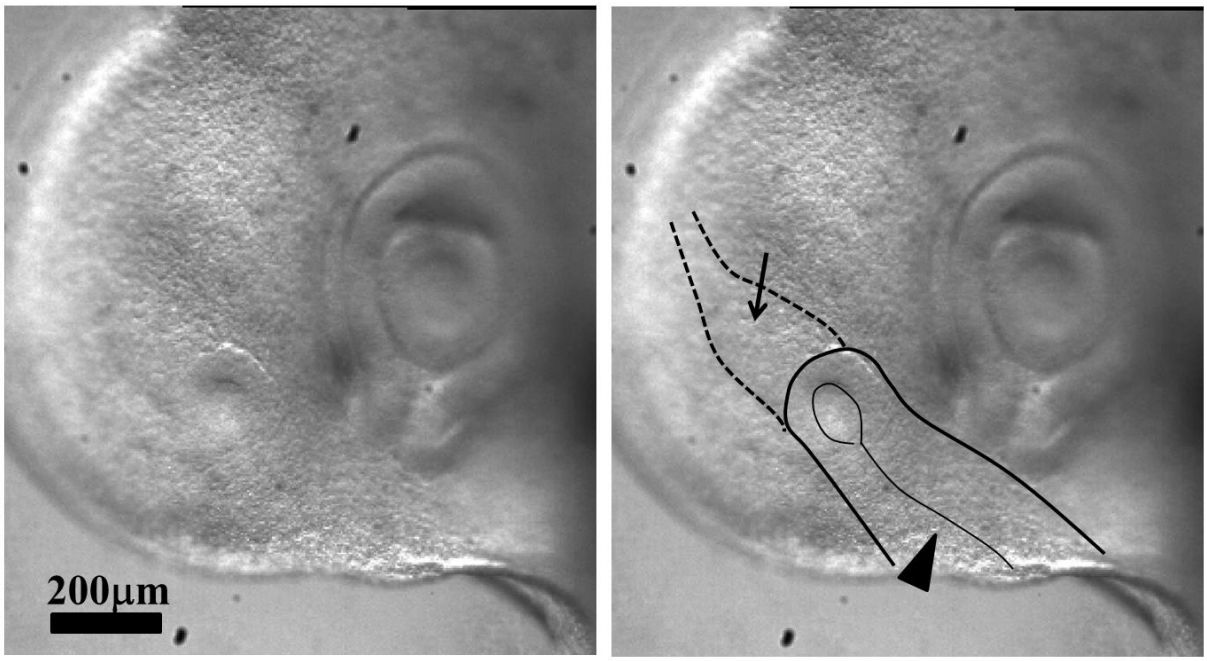

Figure 7B

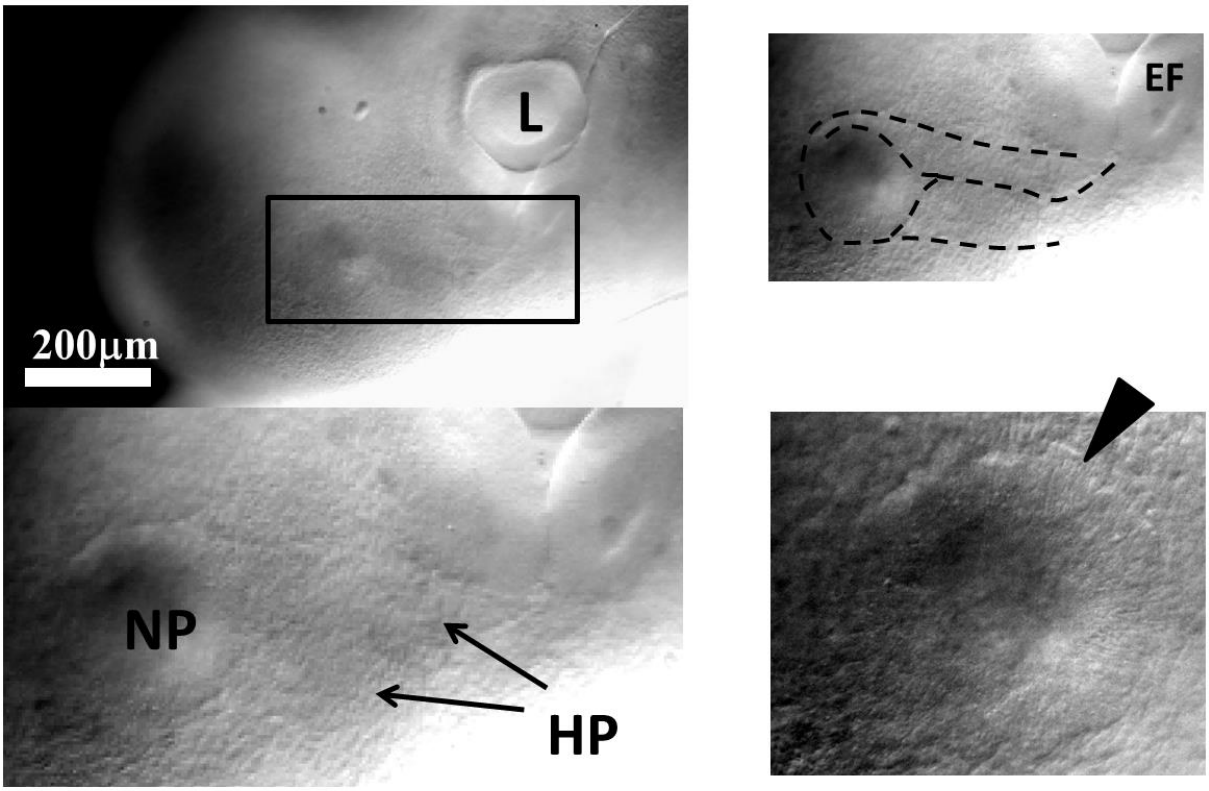

Figure 7C

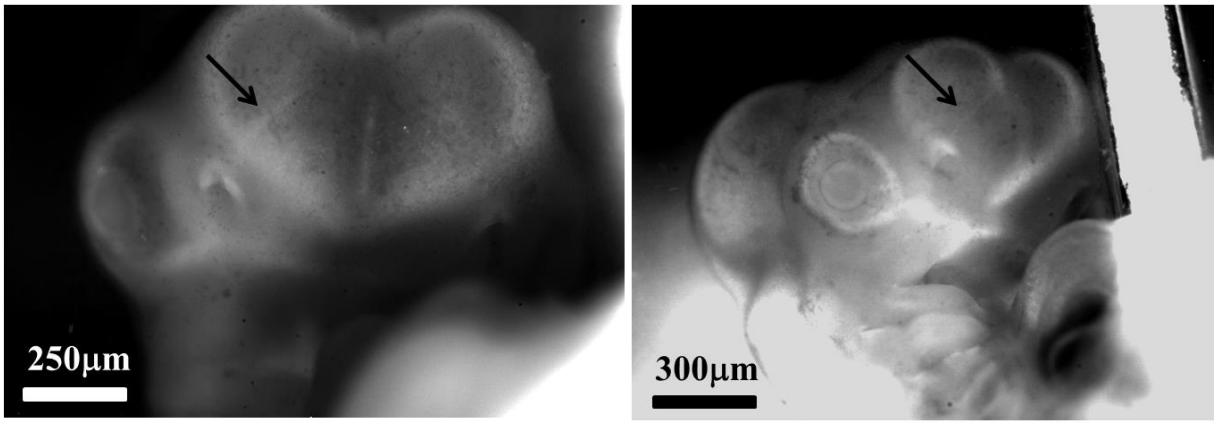

Figure 7D

Figure 7. Formation of the nasal pit. Fig. 7A Formation of the nasal pit as observed at magnification 2X (from Video 15) Formation of the nasal pit is a quite rapid process. After a sudden delamination (see Videos 15-19), the nasal pit becomes well visible in approximately one hour. It is accompanied by complex movements in the oculo-nasal interspace (NP=Nasal Pit; M: Mouth; L: Lens). **Fig. 7B** From Video 17 : During nasal pit formation one observes a sector of tissue visible above the nasal pit (arrow), and a territory in the form of a hairpin around and below the nasal pit (arrowhead). **Fig. 7C** Hairpin of tissue visible below the nasal pit which constricts strongly (see Videos 18, 19 and 20). Along the forming nares, the cells register radially (they stack parallel, black arrowhead); the depth of the nasal pit starts to be visible by topographic contrast in front of the registered cells. The nasal area and the ocular area converge towards the mouth. The oculo-nasal corner where a lacrimal canal

exists in the adult reflects the situation at start (see Fig. 2B and also Videos 2 and 9). (NP=Nasal Pit; EF=Eye Fold; HP=Hair Pin). **Fig. 7D** 24 hours later, the nare is well formed, it has a horseshoe shape and it is connected to the median axis by a thin thread (arrow). The thin thread is associated to a shallow valley on the nasal vesicle (Fig. 7D Right).

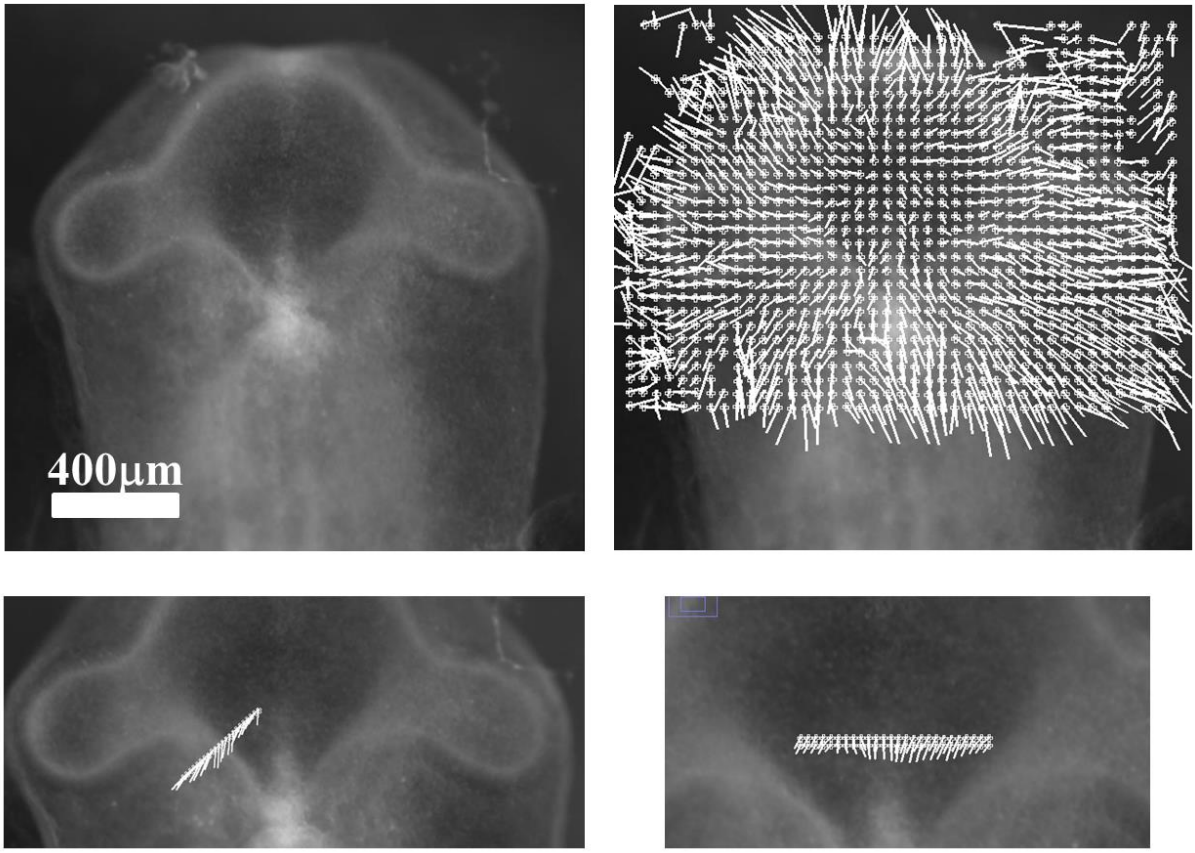

Figure 8

Figure 8. Evidence of a linear force along the lines in the embryo (from Video 13). After closure of the notopore, the brain vesicles balloon out. The PIV map shows a radial expansion of the vesicles. However, if one measures in more detail the speeds perpendicularly to the lines visible on the embryo, one sees that there is a maximum of speed along the lines, with a gradient of displacement away from the lines. This implies a shear force exerted along the lines visible on the embryo head. As the brain vesicle is quasi spherical, gradients in azimuthal movements are actual physical gradients (not projection artefacts).

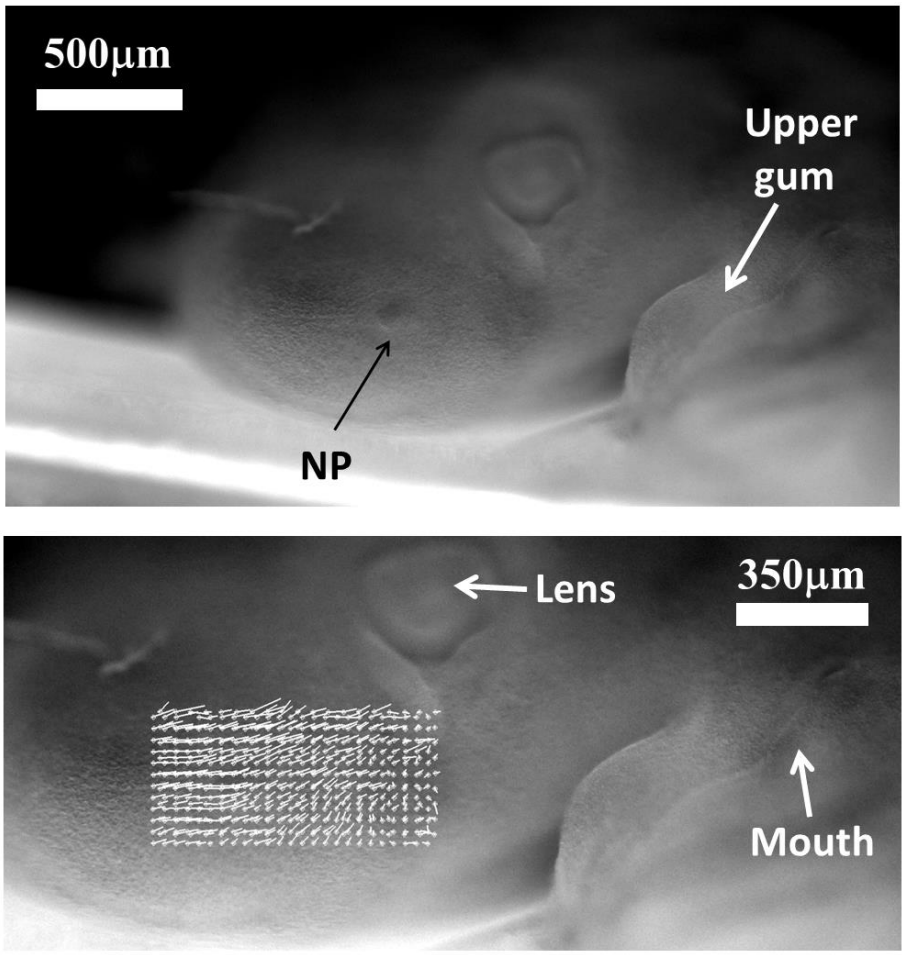

Figure 9A

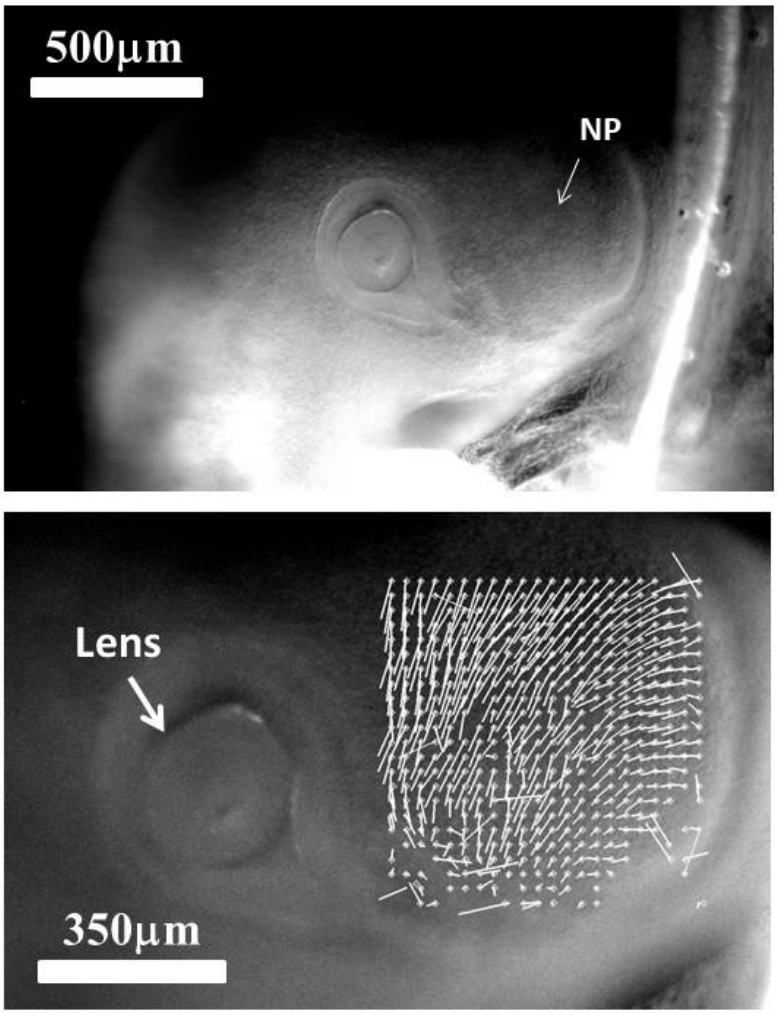

Figure 9B

Figure 9. Spatial analysis of the nasal territory movement. During nares morphogenesis, there exists a movement of the nasal territory towards the eye. The plates 9A and 9B show the movement of the oculo-nasal area (rescaled to visible sizes) extracted by PIV, in the moving frame of the eye. It is seen that the entire presumptive nose territory is dragged towards the eye by a contraction of the oculo-nasal interval. (NP=Nasal placode). Similar movements are very clearly visible in Videos 16 to 20. The close relationship between the nose and the eye originates in the hairpin fold visible in Figs. 2B and 5C.

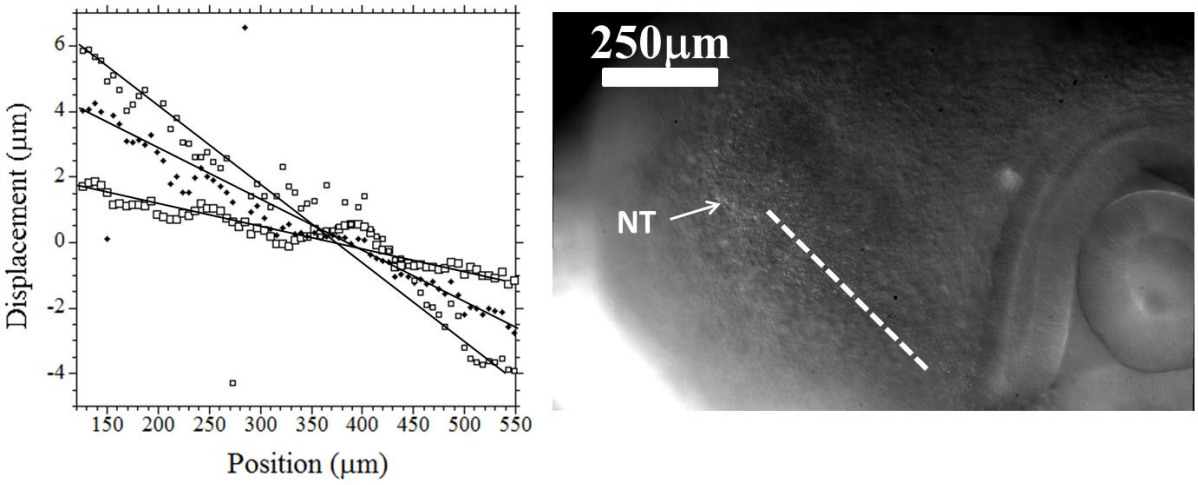

Figure 10A

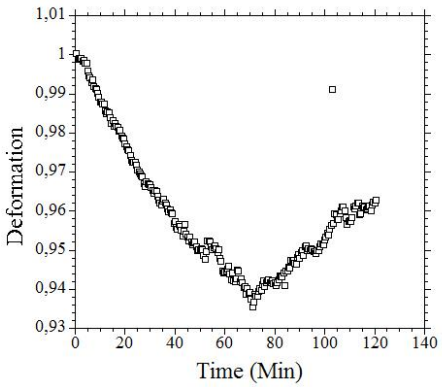

Figure 10B

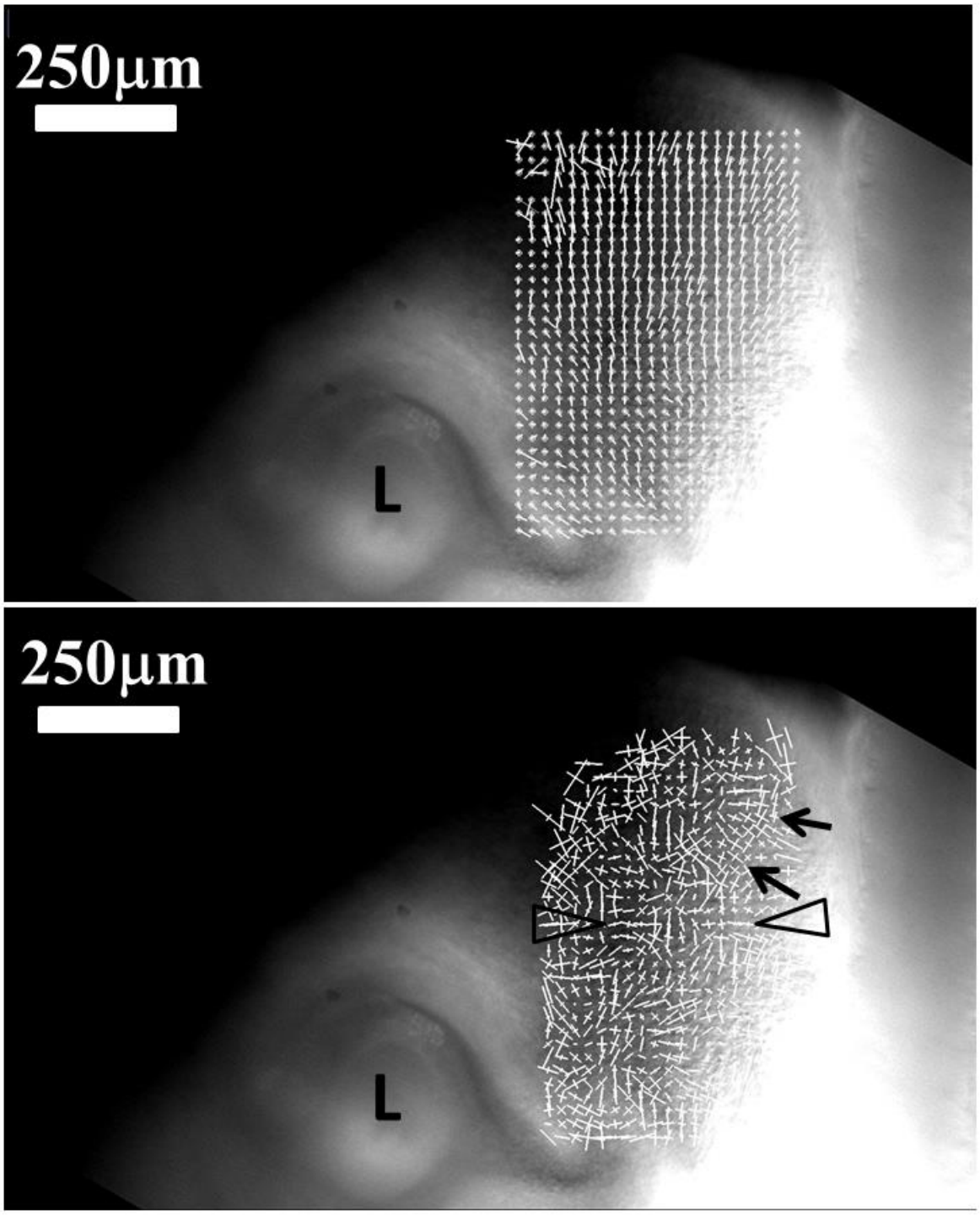

Figure 10c

Figure 10. Quantitative analysis of the oculo-nasal contraction. Fig. 10A. A fine spatio-temporal analysis of the movement in the nasal territory shows a spatial decay (descending slope) of the displacement from the nose towards the eye, revealing that the strain is contractile (a dilational strain corresponds to an ascending slope instead). The temporal variation (3 different times here T0, T0+20Min, T0+40Min.) shows that the strain increases with time (the slope of the gradient of displacement increases), as visually obvious on the Videos 15 to 19. To the right the area of interest, the dashed line shows the segment along which the analysis is done (NT=Nasal Territory). **Fig. 10B** The temporal analysis of the contraction (by following by PIV the distance between a point close to

the presumptive nose, and a point further down the nose sector: the distance shrinks) shows that the contraction increases (the distance between points gets smaller) until there is a sharp relaxation. **Fig. 10C** Analysis of the strain at the beginning of the contraction of the oculo-nasal territory. The top image shows the displacement map, and the bottom image the strain map. The displacement is oriented towards the eye corner. The strain shows a circumferential orientation of the principal strain tensor (arrows) around the presumptive nare (axis aligned radially and orthoradially). Below the presumptive nare, the principal strain tensor is oriented with the long axis perpendicular to the oculo-nasal movement, which means that the tissue is compressed towards the eye corner (not the same embryo as Fig. 10A and B).

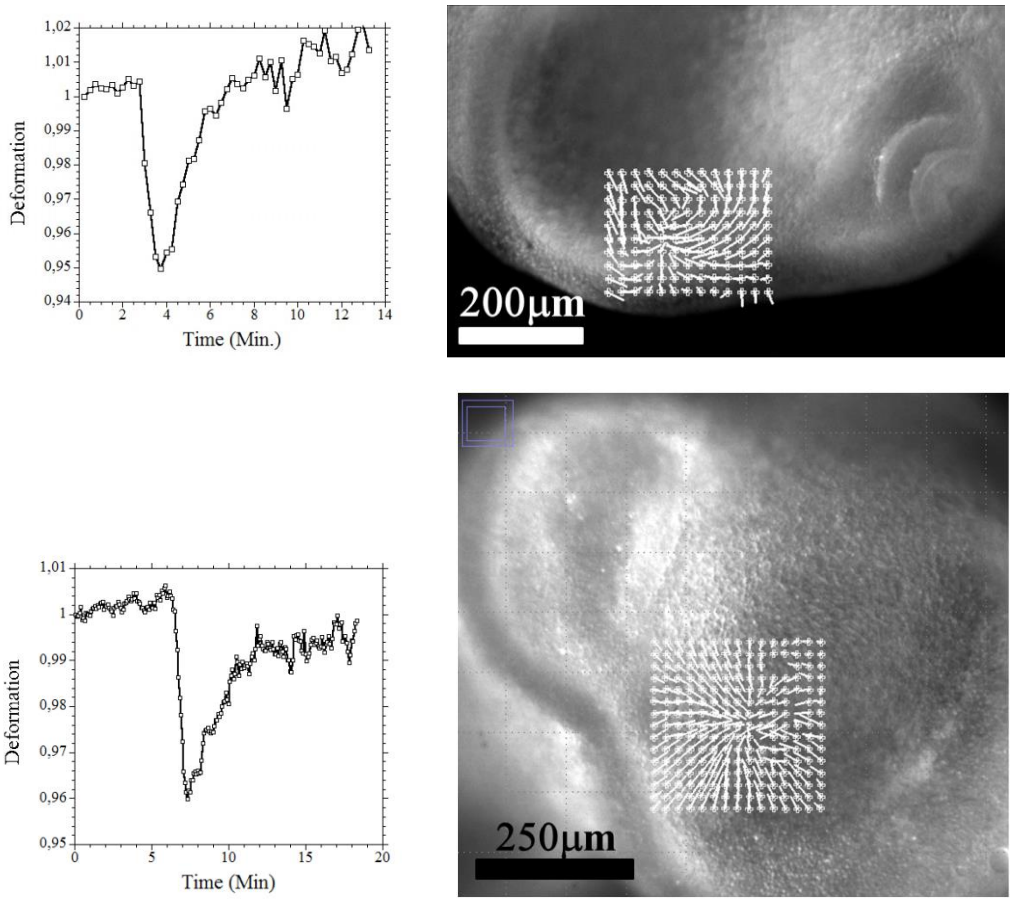

Figure 11A

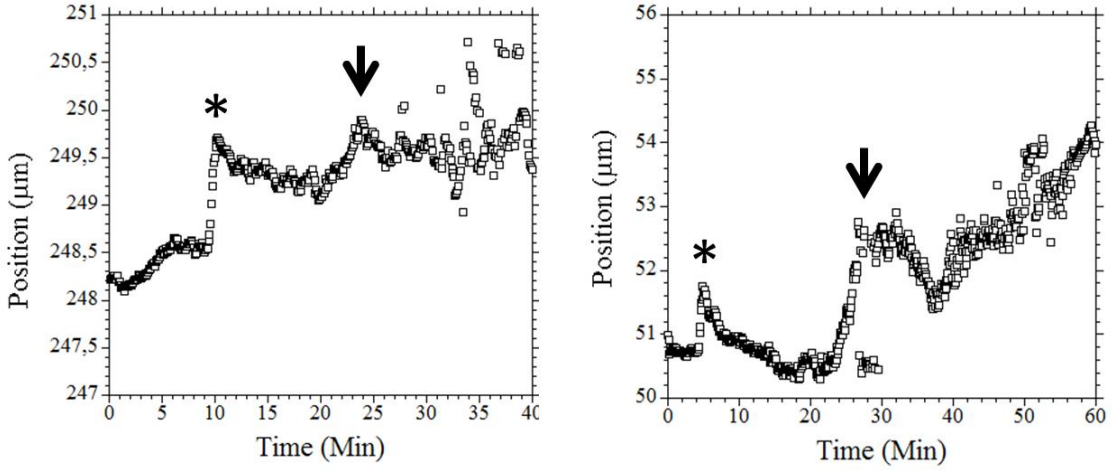

Figure 11B

Figure 11. Excitability of the oculo-nasal tissue. Fig. 11A. The oculo-nasal territory shows sporadic twitches of contraction of amplitude 5% and period 10 Minutes (from Video 23 and another similar Video in a different embryo). The graphs show the temporal behavior of typical contraction twitches, as measured by PIV (by following the distance between reference points), and the images to the right show the foci of movement. The contraction twitches reveal a pattern of relaxation (rapid almost linear contraction followed by a relaxation) intrinsic to the dynamics of the tissue. **Fig. 11B** The contraction twitches are in fact 3D and they flex the ectoderm towards the underneath layers prior to nasal pit formation (see Videos 24, 25). The graph **Fig. 11B left** shows the movement of the neural ectoderm during such a twitch. The first peak (star) shows the direct mechanical effect of the twitch (flexure of the surface, the data shows the depth of the movement, the higher the peak the deeper the flexure), but a detailed PIV monitoring shows that the twitch excites an endogenous response of the neural ectoderm (arrow). (Video 24, 25), while **Fig. 11B Right** shows a similar twitch in the ocular area, prior to lens formation (Video 25, 26).

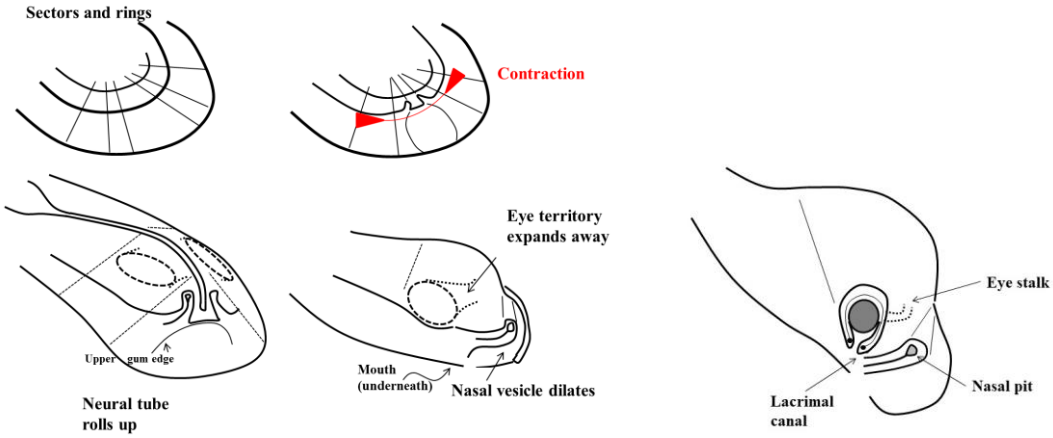

Figure 12A

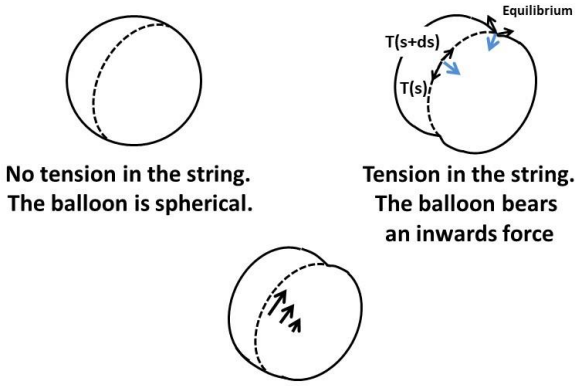

Figure 12B

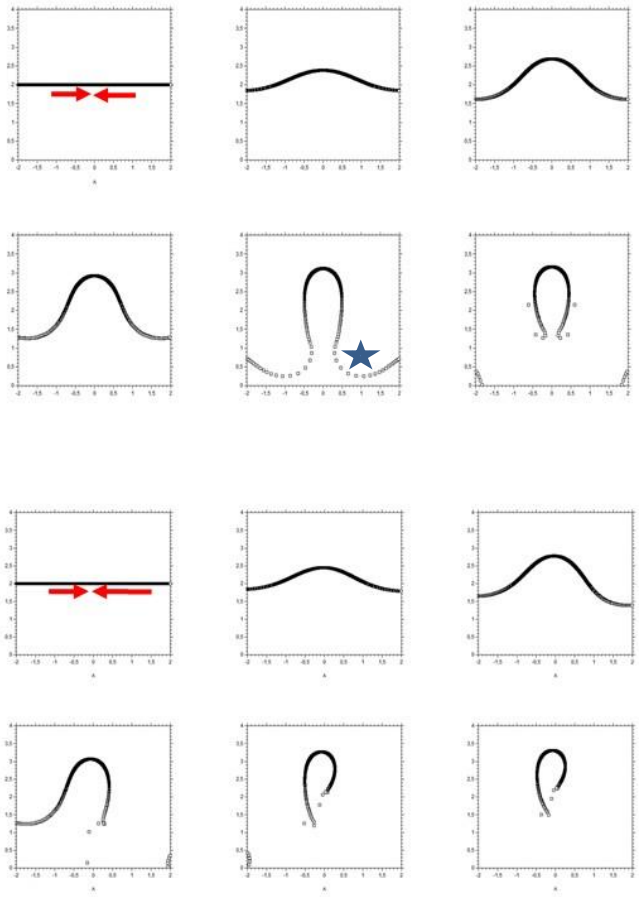

Figure 12C

Figure 12 Mechanism of formation of the nose complex. **Fig. 12A** Initially there is a structure in rings and sectors in the blastodisc (Top Left). The nasal territory and the eye territory are prepatterned by the lines. The D-V boundary contracts in the anterior area, the nasal sector flexes and forms a small hairpin on the surface along the presumptive mouth boundary. It forms an elongated tong of tissue converging towards the median line. During neurulation, the pattern rolls-up (Bottom Left). The front edge flexes down and forms the mouth edge underneath (the gum actually). As the brain vesicles swell, two furrows form on the dilating brain corresponding to the cables locking the eye and nose territories. The eye invaginates: the corner of the eye finds itself directly connected to the basis of the nose territory (Bottom Right). The nose invaginates in a hairpin pattern, because it is a hairpin or horseshoe in the first place. **Fig. 12B** Explanation of the effect of tension in a string or cable acting against dilation of a vesicle. If there is no tension in the string, the surface tension of the balloon is isotropic and the balloon is spherical (Top Left). If there is tension along a string, the line tension induces an inwards force related to the derivative of the tangent vector. (Top Right, blue arrow). This inward force is equilibrated by the inverted curvature of the balloon in the furrow. However, if the tension itself varies, there is an additional tangent force which induces shear (Bottom), this is akin to a Marangoni effect. **Fig. 12C Top** Modelling of horseshoe formation by a

simple viscous potential flow model. We assume that the D-V boundary constricts (quadrupolar system of forces [3]). We assume that the locking by the cables orients the gradient of tension away from the cable (stated otherwise, the cable region is less deformable). If we take a D-V boundary and deform it visco-elastically in a symmetrical contraction force (red arrows of same length), we get a symmetrical winding which tends to form a horseshoe or hairpin (Video 28). **Fig. 12C Bottom** We now assume that the contraction is stronger frontally, since the nose territory is located sideways, where it neighbours the eye territory (see Fig. 2B), we expect the *bilan* of forces to be asymmetrical (asymmetrical red arrows). If we deform a boundary in such an asymmetrical pattern of forces (viscous flow), we form a skewed finger evoking the bent slits seen in the dogfish for example. During formation of the horseshoe, a concavity forms on the other side (star in Fig. 12B Top) which is another niche for possible nare formation, explaining well the situation observed in the thornback ray (Fig. 1B, Bottom). The mathematical model for Fig. 12C is detailed in Ref. 3.

Supplementary Material Methods.

We describe first the preparation of the embryos (Supp. Fig. 2). For study of nasal pit formation, the eggs were most generally incubated in the evening by 6pm so that they were ready for the experiments in the morning of the 3rd day, counting the first day of incubation as zero (for example if eggs are put to incubate on a Friday evening, they are ready on Monday morning, contraction will start by noon, and the nasal pit will form in the afternoon). The shell is broken and the content is dropped into a square plastic cup. If the egg is handled carefully, always keeping the same orientation, the embryo lays generally on top, because of buoyancy of the yolk over the albumin. The embryo is removed from the egg by cutting a round patch of the vitelline membrane around the yolk-sac and embryo (Supp. Fig. 2). These are transferred to a dish with a spoon. There, all the yolk and albumin is rinsed off with Phosphate Buffer Saline (PBS from Dulbecco), and a pipette, and the vitelline membrane is removed with fine tweezers. By day 2.5, the embryo starts to be wrapped by the amniotic sac. In order to improve imaging, the amniotic sac must be removed. In this case, the amniotic sac is torn apart with fine tweezers. The left side of the amniotic sac is more difficult to dissect off being almost stuck to the embryo head. Next the embryo and its yolk-sac are laid flat in a Petri dish, in approximately one centimeter of PBS with the dorsal side down. Next, the anterior part of the yolk-sac is pulled posteriorly with tweezers. By so doing, the head appears now facing the observer, over a dark background. At the end of these steps, the underneath part of the head is more visible, except at stages close to nasal pit formation, when head flexure renders nasal area still more difficult to see. At that stage, we cut a thin plastic thread from a plastic cup (Supp. Fig. 2 Bottom), and slide it gently under the neck, starting from the dorsal side of the neck. By so doing, the head is now lift off slightly, such that the presumptive nasal area appears more clearly. One may think that after all these steps the embryo should be dead. This not the case, and even in the absence of culture medium, the embryo will develop for 6 to 15 hours. It is remarkable how robust the embryos are. The embryo is imaged in white light with a Schott 1500W fiber lamp, either under a binocular (Macrofluo or FLZ III from Leica), or an upright microscope (Nikon Eclipse). A two slits metal plate is used which enhances the contrast by a Mac-Zender type interferometric effect (the two slits system provides a dual light beam, by reflection on the edges, which interfere and increase contrast). The camera was either a monochrome Stingray 200 interfaced with AVT Smartview, or a Basler CMOS camera interfaced with Phase gmbh plugin in ImageJ (ImageJ software from Wayne Rasband), one movie was acquired with an older analog camera from Watek, interfaced with a Scion Frame Grabber DAC board (discontinued). This has allowed me to film the formation of the nasal area starting from the blastula stage. For the sake of completion, and for the final discussion, I give also Videos 12 and 20 which show eye and ear formations as obtained with this technique. The video 20 was presented elsewhere in the context of ear studies [3].

Supplementary Material Figures

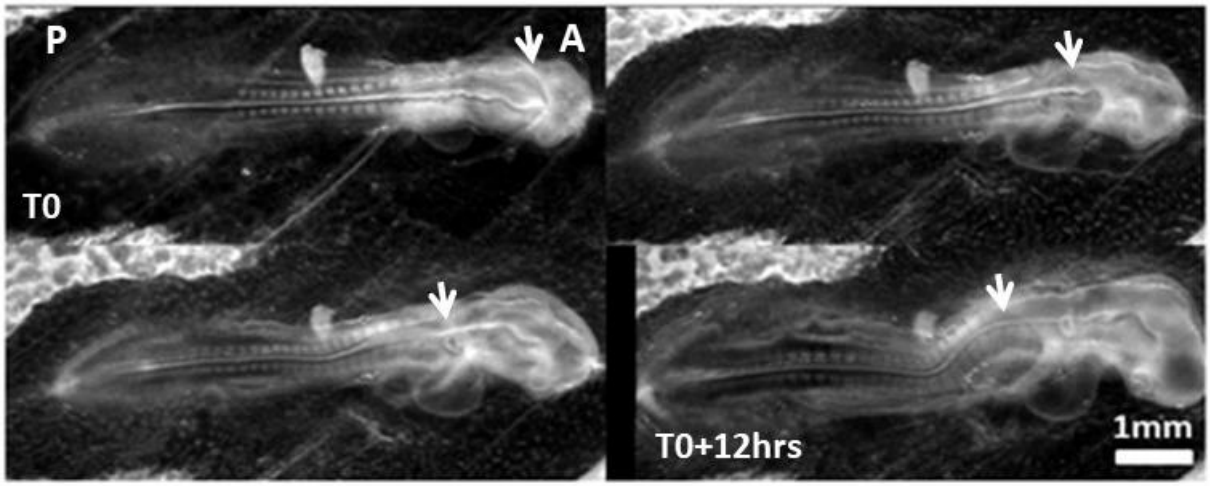

Supplementary Material Figure S1

Supplementary Material Figure S1 Head flexure impedes observation of the nasal territory.

Around the moment of sensory organs formation (HH stages 13-18), the chicken head undergoes a pronounced forward flexure which renders nasal area imaging quite difficult. In addition, the embryo is wrapped by the chorio-amniotic fold (arrows) which blurs the image. This is why the embryo must first of all be removed from the amniotic sac, and next oriented in a different position, in order to get a meaningful image. (A : Anterior ; P : Posterior).

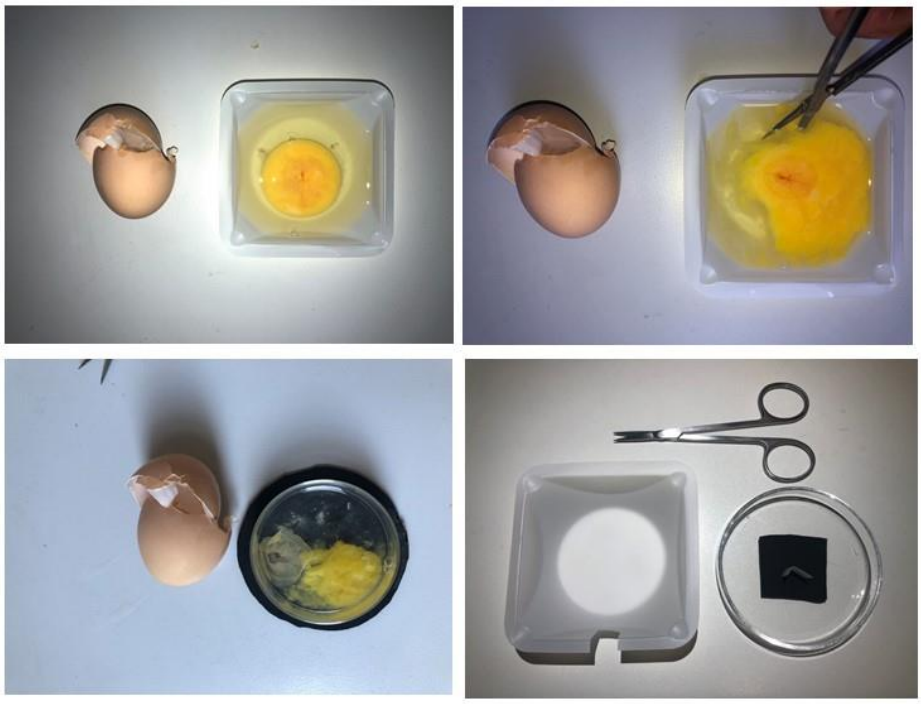

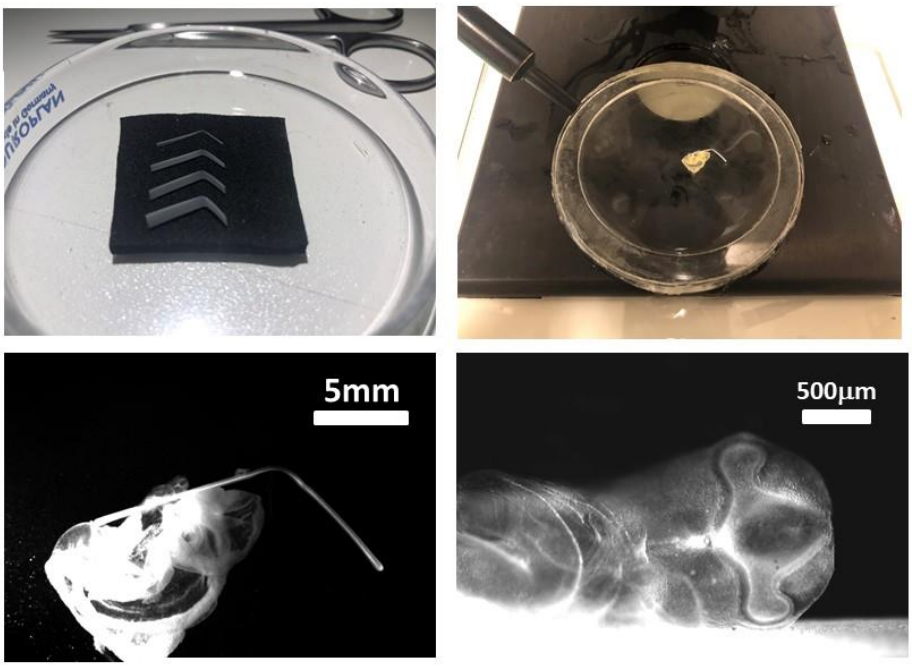

Supplementary Material Figure S2

Supplementary Material Figure S2 Steps in preparing embryos for nasal territory observation. The egg is cracked in a plastic cup. The embryo is cut off and transferred to a Petri dish ; there, it is rinsed. A plastic thread is cut from the angular part of a similar plastic cup. Several threads can be cut, of different widths, to tilt more or less the embryo head. After rinsing, the embryo is turned, the body is lifted and positioned along the edge, so that the head hangs away. This allows one to image more properly the nasal area. Here, the embryo is oriented in a completely frontal view (the embryo is alive, its heart beats properly).

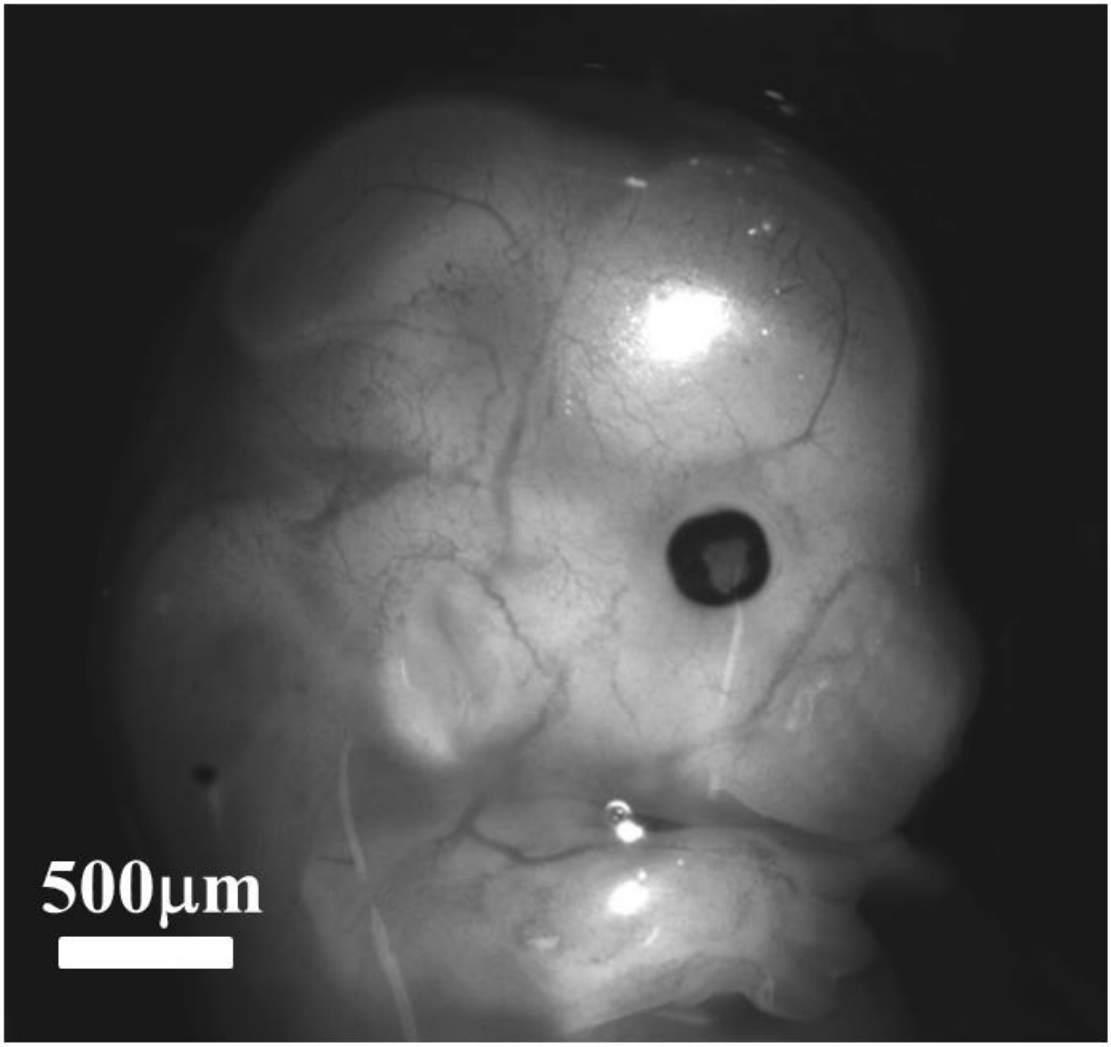

Supplementary Figure S3 During embryo development it is a classical observation that the main blood vessels are positioned in the valleys of the brain vesicles (here a mouse embryo E13.5). Especially, to the right of the eye, one sees the blood vessel which follows the valley separating the ocular territory and the nasal territory.

Supplementary Material Particle Imaging Velocimetry (PIV)

Displacements were extracted from the Time-Lapse videos by Particle Imaging Velocimetry (PIV). PIV is a now classical numerical tool to extract movements [35]. It works by correlation function between selected domains which are tracked from one frame in a stack to the next. Concretely, we have a macro in ImageJ developping language ("Selectagrid") which allows one to generate at will a grid of points with desired spacing. We next apply the plugin "Tracker" (courtesy of O. Cardoso and B. Abou). The "Tracker" pluggin generates by correlation function the file containing the positions (M_x, M_y) of the points as followed in each frame (Lagrangian view of the flow, the data set is the trajectory). From this file we reconstruct the 2D-strain field by calculating the displacements (u_x,u_y) and the components of the strain tensor $\varepsilon_{xx}=\partial_x u_x$, $\varepsilon_{xy}=1/2(\partial_y u_x+\partial_x u_Y)$, $\varepsilon_{yy}=\partial_y u_y$. The 2x2 strain tensor is diagonalized point by point with standard algebra. The eigen vectors correspond to the directions of principal strain, the eigenvalues correspond to principal extensions. A cross is drawn at each point oriented along the principal axis of strain, and the arms of the cross have lengths proportional to the eigen values (length ¾ of the interspacing for an eigenvalue of 1). This plugin (author V. Fleury) is freely available upon request.

Supplementary Material Videos

Video 1 Time lapse video-microscopy of a 2 days embryo observed shell less at low magnification under a binocular. One sees the flexure of the head, the formation of the ear pit and eye, and the chorio-amniotic fold which descends along the body to finally wrap the embryo. Magnification 0.7X, dorsal view, duration 12hours.

Video 2 Time lapse video-microscopy of a 1.5 days embryo observed shell less at magnification 4X. Physiologically the embryo develops the ventral side down. One observes the pull by the primitive streak which triggers the folding of the blastula and chord extension (the morphogenetic force is located dorsally). In the anterior part the eye vesicles appear as the neural folds get into contact. The nasal area is impossible to image in this configuration, since it is located in the anterior part, somewhat ventrally (see Supplementary Fig. 1). The first somites (vertebrate precursors) are visible to the right. If one observes carefully the neural tube, one may see the lines corresponding to the ocular sector which are stretched in the posterior direction. Dorsal view, duration 13hrs.

Video 3 Time lapse video-microscopy of early stage of embryogenesis showing the contraction of the anterior sector of the blastula, prior to neurulation (Mag. 10X, data for Fig. 2). The rings corresponding to the neural territory the dorsal territory, the ventral territory and the extra embryonic organs are clearly visible (white light, no staining). The phenomenon was particularly visible in this embryo. As the mouth sector located to the left in this movie starts to deform in the contraction movement, one may see the two folds which are going, eventually, to form the nares (arrows). (Dorsal view, duration 7 hrs).

Video 4 Time lapse of blastula contraction showing the earliest appearance of the ocular territory at the onset of neurulation (Mag. 4X, data for Fig. 3). The anterior sector will be the mouth sector. The next visible sector is the nasal sector and next the ocular sector. The edge of the mouth sector coincides with the limit of the nasal and ocular territories. To the right a magnified view of the

presumptive ocular area showing the contraction of a horseshoe sector corresponding to the eye territory. (Dorsal view, duration 9 hrs).

Video 5 Beginning of neurulation (Mag. 10X, data for Fig. 4A). Time-lapse showing the edge of the eye sector coinciding with the kink in the neural fold marking the anterior limit of the eye territory (dorsal view, duration 8hrs).

Video 6 Time-lapse video microscopy (Mag. 10X, data for Fig. 4B) of embryo neurulation and early stage of eye stalk extension. By the end of the video the neural crest cells start to migrate. In the first frames one sees the anterior valley or kink in the neural tube corresponding to the limit of the eye territory. (Dorsal view, duration 8hrs).

Video 7 Time-lapse video microscopy (Mag. 10X, data for Fig. 5). Onset of lateral extension of the eye stalk showing the flattening of the presumptive ocular tissue and its lateral winding (dorsal view, duration 2hrs).

Video 8 Time-Lapse video microscopy at Mag. 4X showing the lateral expansion of the eye stalk. (Dorsal view, duration 12hrs).

Video 9 Time-lapse video-microscopy at Mag. 4X showing the lateral expansion of the eye capsule and brain dilation. The nasal territory is found below the eye capsule; this stage is approximately the same as the one in dorsal view in Video 8. (Ventral view, duration 8 hrs).

Video 10 Time-lapse video-microscopy at Mag. 5X and 10X (to the right) showing the thin nasal hairpin between the ocular and oral territories. (Ventral view, duration 8hrs).

Video 11 Time- lapse video microscopy at Mag. 4X showing the lateral expansion of the eye stalk and formation of the eye placode by flattening of the eye stalk against the superficial ectoderm. (dorsal view, duration 4.5hrs).

Video 12 Time-lapse video microscopy at Mag. 10X, around the exact moment of notopore closure showing an acceleration of eye stalk extension and brain vesicle dilation (see Fig. 5B). (Semi-ventro-lateral view, duration 2hrs).

Video 13 Time-lapse video microscopy at magnification 4X showing the ballooning of the brain vesicle as seen from a ventral view (data for Fig. 8). Please note the beginning of the ballooning of the nasal vesicle. (Ventral view, duration 7hrs).

Video 14 Time-lapse video microscopy at magnification 5X of placode invagination forming the eye ball and the lens. One sees that the eye folds have an almond shape oriented frontally towards the nasal and oral area. (Frontal view, duration6hrs).

Video 15 Time-lapse videomicroscopy at magnification 2X of nasal pit formation, as observed “from underneath” with a binocular. One sees movements associated to nasal pit appearance. The pit forms brutally with a nonlinearity associated to apparent stress relaxation (ventral view, duration 8hrs).

Video 16 Time-lapse video microscopy at magnification 3X of nasal pit formation with a binocular (Leica). One sees movements associated to nasal pit appearance. A correlation between the nasal contraction and pit formation is evidenced.

Video 17 Time-lapse video microscopy at magnification 4X of nasal pit formation with a microscope (Nikon Eclipse data for Fig. 7B). One sees movements associated to nasal pit appearance. A correlation between the nasal contraction and pit formation is evidenced, and a sector is evidenced above and below the nare (Profile view, duration 4 hrs).

Video 18 Time lapse video-microscopy at magnification 10X of nasal pit formation with a microscope in white light (Nikon Eclipse, data for Fig. 7C). One sees movements associated to nasal pit appearance. A correlation between nasal contraction and pit formation is evidenced. An elongated territory is observed below the nare with a faintly visible furrow (see fig. 7C). The contracting nasal territory neighbours the eye fold. The territory below the nare will eventually form the lacrimal canal existing between the nose and the eye. This situation originates in the hairpin fold visible in Videos 3 and 10, separating the ocular and nasal territories. (Duration 7hrs).

Video 19 Time-lapse video at magnification 10X of nasal pit formation. One sees a strong contraction of the nasal territory. In this Video, the opening of the nare and invagination of the nare ridge is visible by the end. The nasal sector is visible to the right of the nare (anterior is to the right). (Profile view, duration 5hrs)

Video 20 Close up view of the nare movement after registration of the frames in Video 19. One observes a strong contraction of the nasal territory, which correlates with a radial contraction of the very edge of the nare (narrowing of the ridge), which causes an opening of the nare (widening of the diameter). The superficial ectoderm is seen to invaginate at the ridge edge. (Mag. 10X, duration 5hrs).

Video 21 Time-lapse video microscopy at magnification 4X-10X-4X of ear pit formation, with the same imaging technique. (Dorsal view, duration 10hrs).

Video 22 Time-lapse video microscopy at magnification 4X of neural folds roll-up, in the area of the notopore (concatenates two embryos). The apex of the neural tube forms a U-turn fold which is discussed in the conclusion in reference to the lamprey nasal area. By the end one sees on either side of the eye folds the nasal territory which forms a kink or wedge of tissue (which appears darker because it is thinner), lateral to the closure of the notopore along the median axis (arrow). (Frontal view, duration 10 hours).

Video 23 Endogenous contraction twitch observed in the nasal area prior to nasal pit formation (other examples available, see Fig. 11A). (Semi-frontal/lateral view, duration 30Min.)

Video 24 Endogenous contraction twitch observed in profile view, in the nasal area, just prior to nasal pit formation. The movement shows that the contraction twitch flexes the surface and stimulates the underneath layers (after the flexure, a movement starts underneath). Please magnify the video to full screen to see properly the contraction twitch. (Profile view, duration 30Min.)

Video 25 Endogenous contraction twitch observed in profile view in the ocular area just prior to lens formation. The movement shows that the contraction twitch flexes the surface and stimulates the underneath layers (after the flexure, movement starts in the underneath layer). (Duration 30Min.)

Video 26 Longer Time-lapse showing the onset of invagination, after the contraction twitch (Mag. 4X, Duration 2hrs).

Video 27 Time-Lapse of head flexure at Mag. 4X. Head flexure correlates with mouth invagination (Duration 4 hrs).

Video 28. Animation of a line forming a nasal loop in a viscous flow. A line is advected in a contraction flow formed of two force dipoles oriented “head on”.